

Characteristics analysis of heat and mass transport in catalytic reaction layers of thermally integrated reformers

Junjie Chen¹

¹Department of Energy and Power Engineering, School of Mechanical and Power Engineering, Henan Polytechnic University, Jiaozuo, Henan, 454000, P.R. China. *
Corresponding author, E-mail address: cjtpj@163.com,
<https://orcid.org/0000-0002-4222-1798>

January 22, 2023

Abstract

In conventional fuel cells, a predominantly diffusive heat and mass transport is established in the diffusion layer. However, conventional fuel cells cannot ensure a heat and mass transport from the porous diffusion layer to the catalytic reaction layer that is sufficiently uniform for this purpose. The present study aims to provide a methodology for determining the characteristics of heat and mass transport in catalytic reaction layers. Numerical simulations are performed using computational fluid dynamics to better understand the characteristics of heat and mass transport in catalytic reaction layers of thermally integrated reformers. The present study aims to provide a fundamental understanding of the heat and mass transport in catalytic reaction layers of thermally integrated reformers. Particular emphasis is placed upon the dimensionless quantities involved in thermally integrated reformer with different catalytic reaction layer structures. The results indicate that a vapor-liquid equilibrium exists when the escape tendency of the specie from liquid to a vapor phase is exactly balanced with the escape phase at the same temperature and pressure. It may be beneficial to utilize the thermodynamic work potential provided by the transfer of heat to drive the separation process in the desired direction. If a chamber partition operates below its maximum heat transfer flux capability, this flux often can be increased by augmenting adjacent latent energy transfer which transfers through the partition as sensible energy. The external balance establishes the net enthalpy offset and therefore the temperature difference and the net amount of liquid that may be evaporated or condensed. A pure diffusive heat and mass transport would lead to an uneven reaction density or current density in the catalytic reaction layer, on account of a corresponding lack of uniformity in the heat and mass transport in the same catalytic reaction layer. A high pressure-drop in the thermally integrated reformer is to be avoided, since a high-pressure drop is associated with correspondingly high-power losses, which in turn results in a low overall efficiency. The conduit surface may vary along the general direction of flow to provide the zones either intermittently or preferably continuously as with an undulating membrane surface. When tubular membranes are employed, which membranes are preferably circular in cross section, the zones are preferably provided by circumferential furrowing.

Keywords: Integrated reformers; Temperature differences; Membrane surfaces; Dimensionless quantities; Heat transport; Mass transport

Characteristics analysis of heat and mass transport in catalytic reaction layers of thermally integrated reformers

Junjie Chen

Department of Energy and Power Engineering, School of Mechanical and Power Engineering, Henan Polytechnic University, Jiaozuo, Henan, 454000, P.R. China

* Corresponding author, E-mail address: cjtpj@163.com, <https://orcid.org/0000-0002-4222-1798>

Abstract

In conventional fuel cells, a predominantly diffusive heat and mass transport is established in the diffusion layer. However, conventional fuel cells cannot ensure a heat and mass transport from the porous diffusion

layer to the catalytic reaction layer that is sufficiently uniform for this purpose. The present study aims to provide a methodology for determining the characteristics of heat and mass transport in catalytic reaction layers. Numerical simulations are performed using computational fluid dynamics to better understand the characteristics of heat and mass transport in catalytic reaction layers of thermally integrated reformers. The present study aims to provide a fundamental understanding of the heat and mass transport in catalytic reaction layers of thermally integrated reformers. Particular emphasis is placed upon the dimensionless quantities involved in thermally integrated reformer with different catalytic reaction layer structures. The results indicate that a vapor-liquid equilibrium exists when the escape tendency of the specie from liquid to a vapor phase is exactly balanced with the escape phase at the same temperature and pressure. It may be beneficial to utilize the thermodynamic work potential provided by the transfer of heat to drive the separation process in the desired direction. If a chamber partition operates below its maximum heat transfer flux capability, this flux often can be increased by augmenting adjacent latent energy transfer which transfers through the partition as sensible energy. The external balance establishes the net enthalpy offset and therefore the temperature difference and the net amount of liquid that may be evaporated or condensed. A pure diffusive heat and mass transport would lead to an uneven reaction density or current density in the catalytic reaction layer, on account of a corresponding lack of uniformity in the heat and mass transport in the same catalytic reaction layer. A high pressure-drop in the thermally integrated reformer is to be avoided, since a high-pressure drop is associated with correspondingly high-power losses, which in turn results in a low overall efficiency. The conduit surface may vary along the general direction of flow to provide the zones either intermittently or preferably continuously as with an undulating membrane surface. When tubular membranes are employed, which membranes are preferably circular in cross section, the zones are preferably provided by circumferential furrowing.

Keywords: Integrated reformers; Temperature differences; Membrane surfaces; Dimensionless quantities; Heat transport; Mass transport

1. Introduction

It is of great importance to improve a heat and mass transport in a diffusion layer of a fuel cell [1, 2]. The diffusion layer is connected to a bipolar element which has a plurality of channels for carrying an operating medium [3, 4]. Fuel cells having a diffusion layer and methods of operating such fuel cells are generally known [5, 6]. The operating principle of a fuel cell is based on the principle that in an electro-chemical reaction, namely reactants such as hydrogen and oxygen react to form products such as water [7, 8]. The electrochemical reaction produces a potential difference and an electric current, so that electrical energy can be generated directly by the fuel cell.

A fuel cell includes two catalytic reaction layers which are spaced apart from one another and have a membrane disposed between them [9, 10]. In this case, an anode reaction takes place in one reaction layer and a cathode reaction takes place in the other reaction layer [11, 12]. The membrane ensures a desired transport of charge carriers, for example of protons. Both catalytic reaction layers are operatively connected to in each case one porous diffusion layer, in such a manner that reactants, such as hydrogen and oxygen, and reaction products, for example, water, of the electro-chemical reaction as well as electrons are fed to or removed from the corresponding catalytic reaction layer [13, 14]. In the porous diffusion layer, gas is transported through the pores thereof, while at the same time electrons are transported through the electrically conductive structure of the same diffusion layer [15, 16]. The porous diffusion layer is connected to a bipolar plate or a bipolar element, which on its contact side is provided with channels for carrying an operating medium, which are open at the edges, and webs correspondingly disposed between the channels.

The flow channels in the bipolar plate are used to transport, namely remove or supply, gaseous reactants, namely the starting material or operating medium, and reaction products, while the webs are used in a corresponding manner to supply and remove electrons [17, 18]. In conventional fuel cells, a predominantly diffusive heat and mass transport is established in the diffusion layer [19, 20]. The upper power range of a fuel cell, high current density, is limited by the mass transport of reactants or reaction products through the diffusion layer to or from the catalytic reaction layer and by the transport of waste heat from the catalytic

reaction layer through the diffusion layer [21, 22]. In principle, it is desirable to have a heat and mass transport between the porous diffusion layer and the adjoining catalytic reaction layer that is as uniform as possible [23, 24], in order to achieve a correspondingly uniform reaction density or current density in the same catalytic reaction layer [25, 26]. Conventional fuel cells cannot ensure a heat and mass transport from the porous diffusion layer to the catalytic reaction layer that is sufficiently uniform for this purpose.

The present study is focused primarily upon the characteristics analysis of heat and mass transport in catalytic reaction layers of thermally integrated reformers. Numerical simulations are performed using computational fluid dynamics to better understand the heat and mass transport characteristics. Heat transport, any or all of several kinds of phenomena, is considered as mechanisms, that convey energy and entropy from one location to another. The specific mechanisms are usually referred to as convection, thermal radiation, and conduction. Conduction involves transfer of energy and entropy between adjacent molecules, usually a slow process. Convection involves movement of a heated fluid, usually a fairly rapid process. Radiation refers to the transmission of energy as electromagnetic radiation from its emission at a heated surface to its absorption on another surface. In physics, transport phenomenon is any of the phenomena involving the movement of various entities, such as mass, momentum, or energy, through a medium, fluid or solid, by virtue of nonuniform conditions existing within the medium. Variations of concentration in a medium, for example, lead to the relative motion of the various chemical species present, and this mass transport is generally referred to as diffusion. Variations of velocity within a fluid result in the transport of momentum, which is normally referred to as viscous flow. Variations in temperature result in the transport of energy, a process usually called heat conduction. There are many similarities in the mathematical descriptions of these three phenomena, and the three often occur together physically, as in combustion, where a flowing viscous fluid mixture is undergoing chemical reactions that produce heat, which is conducted away, and that produce various chemical species that inter-diffuse with one another. The present study aims to provide a fundamental understanding of the heat and mass transport in catalytic reaction layers of thermally integrated reformers. Particular emphasis is placed upon the Sherwood and Nusselt numbers involved in thermally integrated reformer with different catalytic reaction layer structures.

2. Methods

Computational fluid dynamics is a common approach for improving the understanding of hydrodynamics, thermodynamics, and chemical kinetics of a flow system [27, 28]. Computational fluid dynamics codes have been evolving over the past two decades [29, 30] with great advances in both the numerical techniques and computer hardware [31, 32]. Computational fluid dynamics applications have been extended from simple laboratory-type problems to complex industrial-type flow systems [33, 34]. Computer simulation has gained widespread acceptance as an effective and cost-saving tool to further improve the performance of flow systems [35, 36]. The present study aims to provide a methodology for determining local kinetic model constants using local fluid dynamic effects in the analysis of chemical flow reactor systems and to extract local chemical kinetic model constants in a reacting flow computational fluid dynamics computer code for a reaction set and reactor system for optimizing system operating parameters and design. The present study also aims to provide an analysis approach which couples computational fluid dynamics with kinetic computations to provide local kinetic constants useful over a broad range of operating conditions for specific and complex reaction sets in specific and complex reactor systems.

The present study contemplates a methodology to extract local chemical kinetic model constants for use in a reacting flow computational fluid dynamics computer code coupled with chemical kinetic computations. obtaining local kinetic model constants as opposed to global model constants is necessary for computing reaction and product yields in non-uniform flow fields under a broad range of operating conditions for a chemical reactor system. A key feature of the methodology is that it uses the coupled computational fluid dynamics and kinetic computer code in combination with data obtained from a matrix of experimental tests to extract the kinetic constants. This approach implicitly includes the local fluid dynamic effects in the extracted local kinetic constants for each particular application system to which the methodology is applied. The application of the methodology does not produce a universal set of kinetic model constants for

a specified set of chemical reactions that will work well in computations for systems that are greatly different in geometry or other significant characteristics. No known method for producing such a set of constants exists, except for very simple reaction sets limited also to relatively simple reactor systems. The present methodology provides a means to extract local kinetic model constants that work well over a fairly broad range of operating conditions for specific and complex reaction sets in specific and complex reactor systems. Once the kinetic model constants are extracted for a reaction set and reactor system, the model constants can be used in the coupled computational fluid dynamics and chemical kinetic code to optimize the operating conditions or design of the system, including planned retrofit design improvements to existing systems.

The local kinetic model constant extraction methodology requires the use of a computational scheme for coupling computational fluid dynamics calculations with chemical kinetic calculations in a novel two stage approach that avoids numerical stiffness problems that frequently arise when computational fluid dynamics and chemical kinetic computations are coupled. The computer code in which this two-stage approach is implemented and used to test the methodology is a computational fluid dynamics program. Boundary conditions consist of flow inlets and exit boundaries, wall, repeating, and pole boundaries, and internal face boundaries. Velocity inlet boundary conditions are used to define the velocity and scalar properties of the flow at inlet boundaries. Pressure inlet boundary conditions are used to define the total pressure and other scalar quantities at flow inlets. Mass flow inlet boundary conditions are used in compressible flows to prescribe a mass flow rate at an inlet. It is not necessary to use mass flow inlets in incompressible flows because when density is constant, velocity inlet boundary conditions will fix the mass flow. Like pressure and velocity inlets, other inlet scalars are also prescribed. Pressure outlet boundary conditions are used to define the static pressure at flow outlets and also other scalar variables, in case of backflow. The use of a pressure outlet boundary condition instead of an outflow condition often results in a better rate of convergence when backflow occurs during iteration.

Pressure far-field boundary conditions are used to model a free-stream compressible flow at infinity, with free-stream Mach number and static conditions specified. This boundary type is available only for compressible flows. Outflow boundary conditions are used to model flow exits where the details of the flow velocity and pressure are not known prior to solution of the flow problem. They are appropriate where the exit flow is close to a fully developed condition, as the outflow boundary condition assumes a zero streamwise gradient for all flow variables except pressure. They are not appropriate for compressible flow calculations. Inlet vent boundary conditions are used to model an inlet vent with a specified loss coefficient, flow direction, and ambient or inlet total pressure and temperature. Intake fan boundary conditions are used to model an external intake fan with a specified pressure jump, flow direction, and ambient or intake total pressure and temperature. Outlet vent boundary conditions are used to model an outlet vent with a specified loss coefficient and ambient or discharge static pressure and temperature. Exhaust fan boundary conditions are used to model an external exhaust fan with a specified pressure jump and ambient or discharge static pressure. Wall boundary conditions are used to bound fluid and solid regions. In viscous flows, the no-slip boundary condition is enforced at walls by default, but you can specify a tangential velocity component in terms of the translational or rotational motion of the wall boundary, or model a slip wall by specifying shear.

3. Results and discussion

The Sherwood number profiles along the length of the thermally integrated reformer with a continuous catalytic reaction layer structure are presented in Figure 1 at different velocities of flow at the reactor inlet. Dimensional consistency is required when computing formulas using dimensional quantities. For example, when adding two dimensional quantities together, both dimensional quantities must represent the same kind of dimensional measurement. Dimensional consistency requires knowing not just the units of measure used for the input dimensional quantities, but also the kind of measurement each unit refers to. Through the use of a gas which is generally defined as a noncondensing vapor or gas and in most cases is ambient air. This gas generally flows through a chamber which is thermally connected to a heat sink and in one case a heat source. Thermally connected, in this context, means that fluids from a chamber are brought into close proximity of a heat transferring barrier so that heat can transfer from a chamber to a sink or from a source to a chamber.

In its passage, the gas generally operates under nearly constant pressure with pressure changed caused by frictional losses. The heat sources and sinks being of different temperature than the gas in the chamber cause a temperature and absolute humidity change to be created in the gas from one end of the chamber to the other. These changes cause the gases to approach a vapor-liquid equilibrium value and be thus receptive to receiving or losing vapors. Equilibrium value is a vapor-liquid equilibrium concentration or temperature. A vapor-liquid equilibrium exists when the escape tendency of the specie from liquid to a vapor phase is exactly balanced with the escape phase at the same temperature and pressure. In operation, where there is evaporation from the wetting desiccant into the gas stream or selective condensation from this gas stream, segmented wetting coupled with migratory movement provide the following occurrences. First, as a sector is wetted by primarily the same wetting desiccant, the now localized wetting desiccant temperature and composition can be forced to change. Second, as the migratory movement is from one sector to another, the concentration of one sector influences the wetting desiccant composition of the subsequent sector where it again may be altered by evaporation or condensation. In this manner, selected desiccant property gradients can be developed and maintained throughout the chamber length. The apparatus consists of a chamber and heat sink which generally is found throughout the chamber length. A gas is moved into the chamber by mechanical means which can be a low-pressure blower. Multiple liquid segmentations generally caused by segregated pumping and distribution means are provided. This distribution generally encompasses wetting of the heat sink barrier, but may further include wetting methods to increase chamber gas and wetting desiccant contact area, for example, the use of droplet sprays. The number of segmentations is sufficient to allow the wetting desiccant temperature to approach the temperatures of the passing gas proximate thereto and also present any significant concentration variances developed within the wetting desiccant.

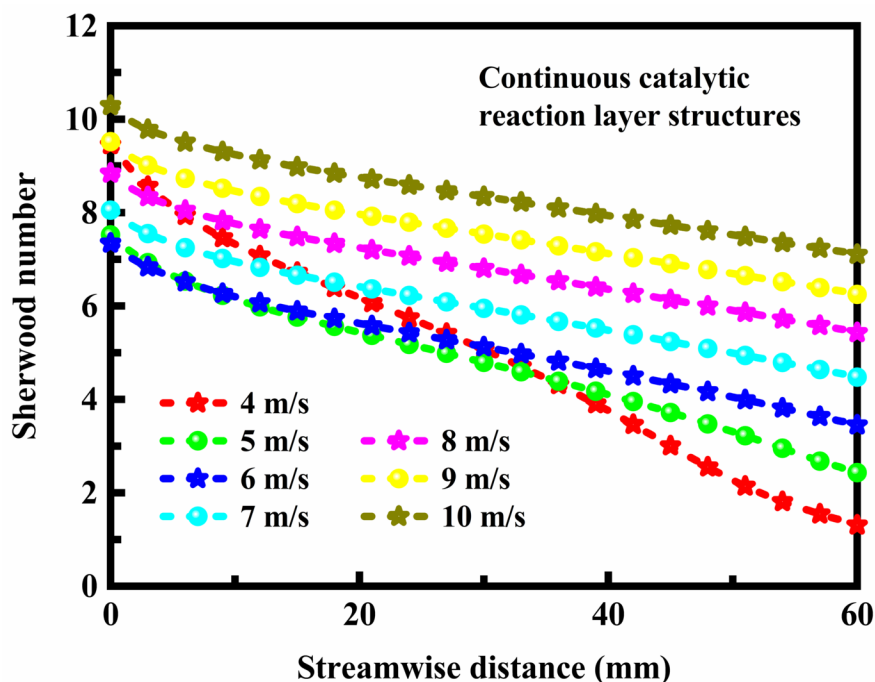


Figure 1. Sherwood number profiles along the length of the thermally integrated reformer with a continuous catalytic reaction layer structure at different velocities of flow at the reactor inlet.

The Sherwood number profiles along the length of the thermally integrated reformer with a segmented catalytic oxidation reaction layer structure are presented in Figure 2 at different velocities of flow at the reactor inlet. Mass exchange between two phases is of particular importance largely because it is involved in most separation processes, as for example in the recovery of a pure product from a mixture [37, 38]. Most

practical schemes are based on the fact that concentrations of two phases in equilibrium with each other are quite different [39, 40]. Any method of contacting two phases which results in the selective interphase transport of one of the constituents can form the basis of a separation process [41, 42]. The selectivity can be the result of different equilibrium composition for the different species or it may be due to different rates of transport of the several constituents [43, 44]. Thermodynamic work potential of several kinds may serve to implement mass exchange. In electrochemical processes, an electrical potential provides the motive force, while in a column for the separation of gaseous isotopes, it is a thermal gradient [45, 46]. However, in the majority of applications in the process industries, it is the concentration gradient which provides the driving force to effect mass exchange between two phases. This is a well-established operation carried generally in a multi-stage operation such as in distillation towers, mixer-settler units, and is based on well-known theory. Thermodynamic considerations require that work be invested in a system in order for its components to be separated, involving a decrease in entropy. Heat transfer between a relatively hot body and a relatively cold body is also a well-established unit operation that is carried in a variety of devices such as heat exchangers and heat regenerators. It may be beneficial to utilize the thermodynamic work potential provided by the transfer of heat, whereby the hot input stream is tagged as a heat source and the cold input stream is tagged as a heat sink, to drive the separation process in the desired direction, the entire process occurring in one operation. This integration may be beneficial both from the point view of energy utilization and by virtue of the compactness of the equipment which would perform two functions simultaneously, for example, in catalytic reaction layers of thermally integrated reformers. The overall efficiency of the process will depend on a number of factors such as: the amount and adsorbing power of the adsorbing reagent as a function of temperature; the heat capacities of the adsorbing reagent and of the fluids; flow rates, temperatures and compositions of the inlet streams and the thermodynamical properties of the materials involved.

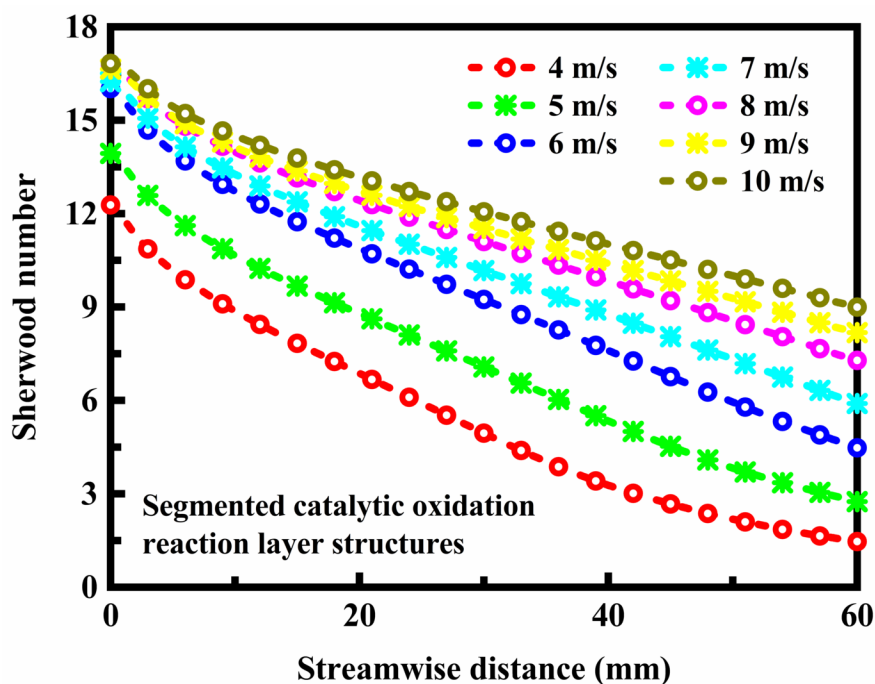


Figure 2. Sherwood number profiles along the length of the thermally integrated reformer with a segmented catalytic oxidation reaction layer structure at different velocities of flow at the reactor inlet.

The Sherwood number profiles along the length of the thermally integrated reformer with a segmented catalytic reforming reaction layer structure are presented in Figure 3 at different velocities of flow at the reactor inlet. The design can be presented in terms of heat transfer and mass and energy balances. The

conduction of energies between chambers always involves sensible heat and, generally, at least one latent heat transfer related to evaporation or condensation. Sensible heat is that heat required to change the temperature of a substance without changing the state of the substance. Latent heat is that heat required to change the state of the substance from solid to liquid or from liquid to gas without change of temperature or pressure. A basic heat transfer is established by the auxiliary heat exchange to the gas before this gas returns to the second chamber. This exchange causes a temperature differential between the gas in each chamber. In order to preserve this temperature differential along the chamber lengths, the gases are made to flow in a thermally counter-current direction in the first and second chambers. This thermally counter-current gas movement results from the thermal connection between the sequentially ordered sectors of the first and second chambers by means of the heat transferring partitions. The continually changing temperatures of the gas within the chambers cause a continual shifting of the vapor-liquid equilibrium value between the liquid and gas phases. This shifting allows evaporation and condensation between the moving gas and the wetting substances. The energies released in condensation are normally transferred to the other chamber allowing for additional evaporation to occur from the wetting substances. Where many sectors are wetted, as in the case of the concentration and fractionation modes, these transfers of latent energy are many times the sensible energy related to the temperature change of the gas. This sensible exchange, in turn, is greater than any auxiliary heat exchange into the gas. In other operating modes, the latent energies associated with evaporation from the segmented wetting substances can be turned to sensible energies in that such evaporation can cause the gas to further lower in temperature. Generally speaking, minimum wetting substance movement occurs when energy transfer between chambers involves exchange directly through wetted partitions separating the chambers. However, there are occasions when this minimum is balanced against other rates. One concern is the rate of energy conducting through a certain partition area including liquids on the partition, called the partition heat transfer flux. The partition heat transfer flux is maximized if the temperature difference across the partition is increased to a maximum value of the specified temperature differential between chambers. If a chamber partition operates below its maximum heat transfer flux capability, this flux often can be increased by augmenting adjacent latent energy transfer which transfers through the partition as sensible energy. This augmentation involves inclusion of additional gas-liquid heat transfer contact area beyond that supplied by wetting the partition, for example, by the use of spray droplets within the chamber area. This expansion of latent transfer surface is useful. Conversely, in other cases such as some concentration operations, latent transfer within the chambers is capable of being in excess of the maximum partition flux. When both chambers are segmented wetted, an increased partition area can be supplied by thermally connected partitions that are external to the chambers. In this manner, the partition heat transfer flux can operate at its maximum along with increased chamber sensible and latent heat transfer.

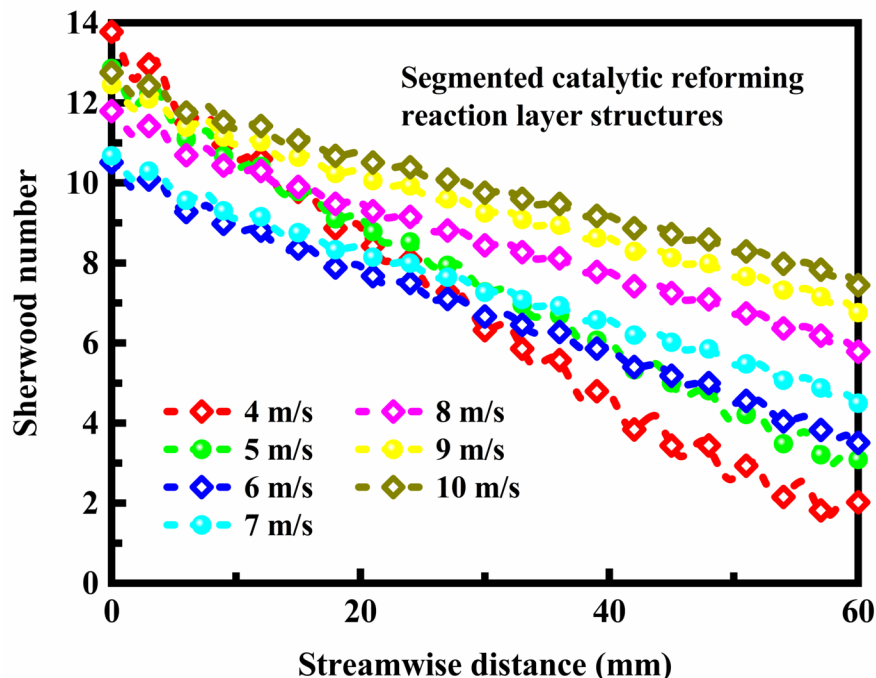


Figure 3. Sherwood number profiles along the length of the thermally integrated reformer with a segmented catalytic reforming reaction layer structure at different velocities of flow at the reactor inlet.

The Sherwood number profiles along the length of the thermally integrated reformer are presented in Figure 4 with different catalytic reaction layer structures. A net overall mass and energy balance encompassing the entire process includes the enthalpy of the incoming gas plus the input energy to this gas from an auxiliary heat exchange all being equal to the enthalpy of the exiting gas. In some modes of operation, there is also the enthalpy of a feed material and the enthalpy of a product material, as for example in concentration which may involve an incoming brackish water and products of substantially pure water and brine concentrate. The energy associated with these feeds and products tends to either cancel or be made inconsequential. The above energy balance reveals that where both gas streams are saturated and the auxiliary heat exchange adds energy, for example in the concentration and fractionation modes, there would be a shift in temperature of those gas streams in the same direction as the shift in enthalpies. In this way the gas stream with the highest enthalpy and highest temperature would be associated with the cooling or condensing chamber allowing its energy to be transmitted to the lower enthalpy and lower temperature gas stream located in the heating or evaporation chamber and thereby reused. Owing to the differences in saturation, there can be a shift in temperature of those gas streams in the opposite direction as the shift in enthalpies. The gas stream with the lowest enthalpy but highest temperature would be associated with the cooling chamber allowing its energy to be transmitted to the higher enthalpy but lower temperature gas stream located in the second chamber. In summary, the external balance establishes the net enthalpy offset and therefore the temperature difference between the two chambers and the net amount of liquid that may be evaporated or condensed. An internal chamber energy balance gives detail on the actual amount of temperature rise or fall in a chamber and on the actual amount of liquid evaporated or condensed in a chamber. An internal mass and energy balance around a chamber equates the incoming gas enthalpy to a chamber plus the conducting energies associated with the partition to the exiting gas enthalpy from a chamber. The two forms of conducting energies are sensible energy needed to heat up or cool down chamber gas, and latent energy needed for evaporation or condensation into or out of the chamber gas. The internal chamber balance also relates the chamber exiting gas temperatures to the amount of sensible and latent energies that can transfer to the gas in a chamber. The more energies that can transmit to the chamber gas the larger will be the temperature rise and fall

and actual evaporation into or actual condensation out of the chamber gas from the chamber entrance to chamber exit.

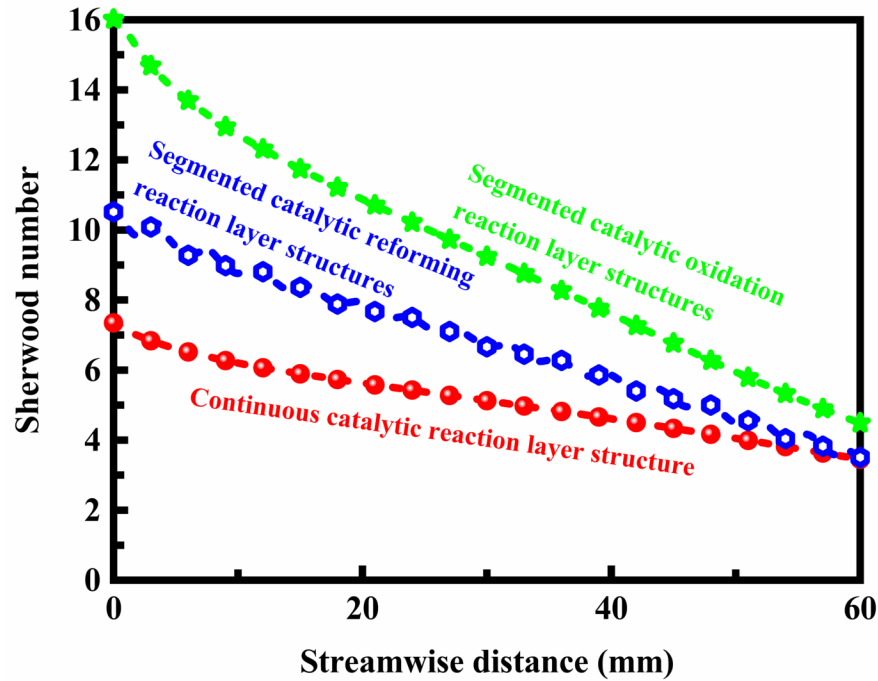


Figure 4. Sherwood number profiles along the length of the thermally integrated reformer with different catalytic reaction layer structures.

The Nusselt number profiles along the length of the thermally integrated reformer with a continuous catalytic reaction layer structure are presented in Figure 5 at different velocities of flow at the reactor inlet. The diffusion layer is connected to a bipolar element which includes a plurality of channels for carrying an operating medium. The heat and mass transport in a diffusion layer is characterized in that a pressure difference is generated in at least two adjacent channels for carrying operating medium, so as to form a convective heat and mass transport. A pressure difference is generated in at least two adjacent channels for carrying an operating medium, so as to form a convective heat and mass transport. In this context, a distinction needs to be drawn between a diffusive and a convective heat and mass transport. A diffusive transport is established on account of the existence of a concentration gradient or a temperature gradient, while a convective transport is attributable to the presence of a pressure gradient. Therefore, both a diffusive heat and mass transport and a corresponding convective heat and mass transport are produced, since there is a sufficiently great pressure gradient between at least two adjacent channels for carrying an operating medium. A pure diffusive heat and mass transport would lead to an uneven reaction density or current density in the catalytic reaction layer, on account of a corresponding lack of uniformity in the heat and mass transport in the same catalytic reaction layer. A reaction density or current density which is more uniform compared to the previous designs can be achieved in the catalytic reaction layer by the convective heat and mass transport which is additionally established in accordance with the design. In this context, the term adjacent channels for carrying an operating medium can also be understood as meaning corresponding channel sections that are adjacent to one another.

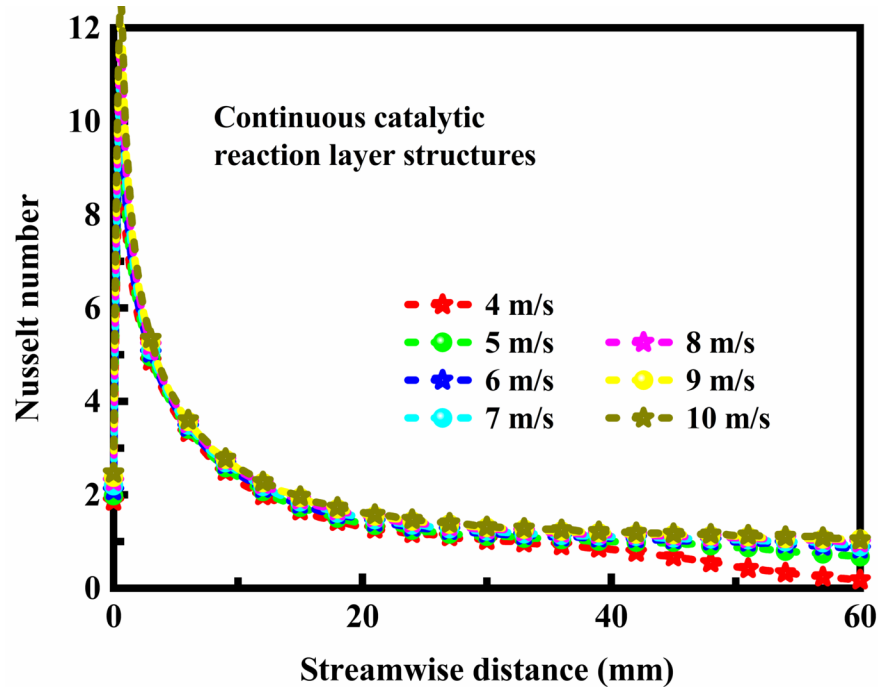


Figure 5. Nusselt number profiles along the length of the thermally integrated reformer with a continuous catalytic reaction layer structure at different velocities of flow at the reactor inlet.

The Nusselt number profiles along the length of the thermally integrated reformer with a segmented catalytic oxidation reaction layer structure are presented in Figure 6 at different velocities of flow at the reactor inlet. The operating medium advantageously includes gaseous reaction products and gaseous reactants or reaction starting materials. The reaction products may be water and the reaction starting materials or reactants may be hydrogen and oxygen, which are each carried through the channels for carrying an operating medium in the gaseous state. Accordingly, hydrogen and oxygen are transported as reactants in the diffusion layer. The substances which are to be transported in the diffusion layer are preferably reactants, in particular hydrogen and oxygen, reaction products, in particular water, and electrons [47, 48]. The use of these substances in a fuel cell is already known [49, 50]. These substances are transported from the diffusion layer to a catalytic reaction layer of the thermally integrated reformer. The gaseous reactants are supplied as pure reactants or as part of a mixture [51, 52]. The bipolar element is preferably configured as a surface-structured bipolar plate with, on one surface, channels for carrying an operating medium, which are open at the edges, and webs disposed between them. The channels for carrying the operating medium are used to supply and remove the gaseous reactants and reaction products, while electrons are correspondingly supplied and removed via the webs. Gaseous reaction products and reaction starting materials, and also electrons, pass into the diffusion layer [53, 54]. In other words, the surface-structured bipolar plate has a surface formed with webs between the channels, which are open at the surface of the bipolar plate [55, 56]. The pressure difference is generated in each case in two adjacent channels for carrying the operating medium and, at the same time, the pressure drop between an operating-medium inlet and an operating-medium outlet of the thermally integrated reformer is minimized. A high pressure drop in the thermally integrated reformer is to be avoided, since a high-pressure drop is associated with correspondingly high-power losses for example in compressors which in turn results in a low overall efficiency. Therefore, a pressure difference between two adjacent channels for carrying an operating medium is particularly desirable, however, at the same time, a low pressure drop with regard to the thermally integrated reformer as a whole should be provided.

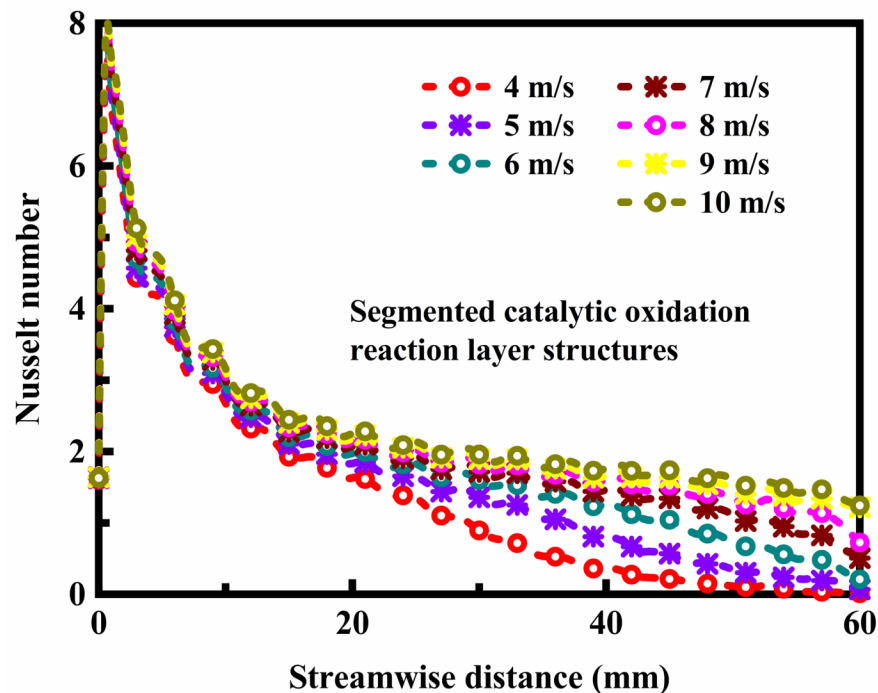


Figure 6. Nusselt number profiles along the length of the thermally integrated reformer with a segmented catalytic oxidation reaction layer structure at different velocities of flow at the reactor inlet.

The Nusselt number profiles along the length of the thermally integrated reformer with a segmented catalytic reforming reaction layer structure are presented in Figure 7 at different velocities of flow at the reactor inlet. Macroscopic description of porous media is based on two basic assumptions: continuous medium approximation, which disregards microscopic structure of the material and assumes continuous distribution of the matter in space, and phenomenological response coefficient approximation, which disregards internal degrees of freedom of the material and assumes that the material responds to the external force, such as temperature or pressure gradient and electric potential, as an unstructured entity with certain response coefficient, such as thermal conductivity, permeability, and electric conductivity [57, 58]. Since macroscopic modeling is a primary tool in many industrial and scientific applications, the microscopic modeling is often considered an auxiliary tool for estimating the macroscopic response coefficients [59, 60]. However, the macroscopic models are insufficient. One-phase macroscopic fluid transport model is based on permeability coefficient [61, 62]. It is well known, that a rather extensive set of one-phase transport phenomena lies outside the permeability coefficient concept [63, 64]. Multiphase fluid transport model is based on phase permeability coefficients, and this approach is insufficient and microscopic processes are important [65, 66]. The conduit configuration varies periodically along the general direction of flow, either inherently or in response to fluid pressure therein, in order to give rise to separation and reattachment of the flow at a multiplicity of zones within the conduit whereby secondary flow is induced within the zones. The zones which can vary considerably in configuration are generally spaced one from another by constrictions to flow through the conduit. When fluid is pulsated across a constriction, the flow is detached therefrom and re-attaches at a neighboring constriction with eddy formation in the zone between the constrictions. The eddies which reduce the boundary layer effect generally take the form of vortices, the axes of which are transverse to the general direction of flow. The conduit surface, typically the surface of the membrane, may vary along the general direction of flow to provide the zones either intermittently or preferably continuously as with an undulating membrane surface. The zones may take a variety of configurations. In particular, they may extend across the surface of the conduit transverse to the direction of flow to provide furrows or may be present as local depressions such as dimples in a conduit surface, such depressions preferably having

curved bases and conveniently being hemispherical. When the surface of the membrane is shaped into zones in response to the pressure of fluid in the conduit, one or more means are provided associated with the membrane for constraining the latter to adopt the required configuration in response to the pressure of fluid therein. However, zones may be provided in the region of the membrane surface by a shaped member within the conduit and conveniently formed prior to insertion therein. The membrane itself is conveniently tubular and the means for constraining the fluid flow in a helical path may be formed by twisting a strip of material about its longitudinal axis to provide an insert which preferably fits tightly inside the tube. When fluid in pulsated in the conduit, secondary rotary flow is induced in the fluid the axis of which lies generally in the direction of flow. Such secondary flow enhances the mixing action promoted by the helical fluid motion and facilitates transfer through the membrane.

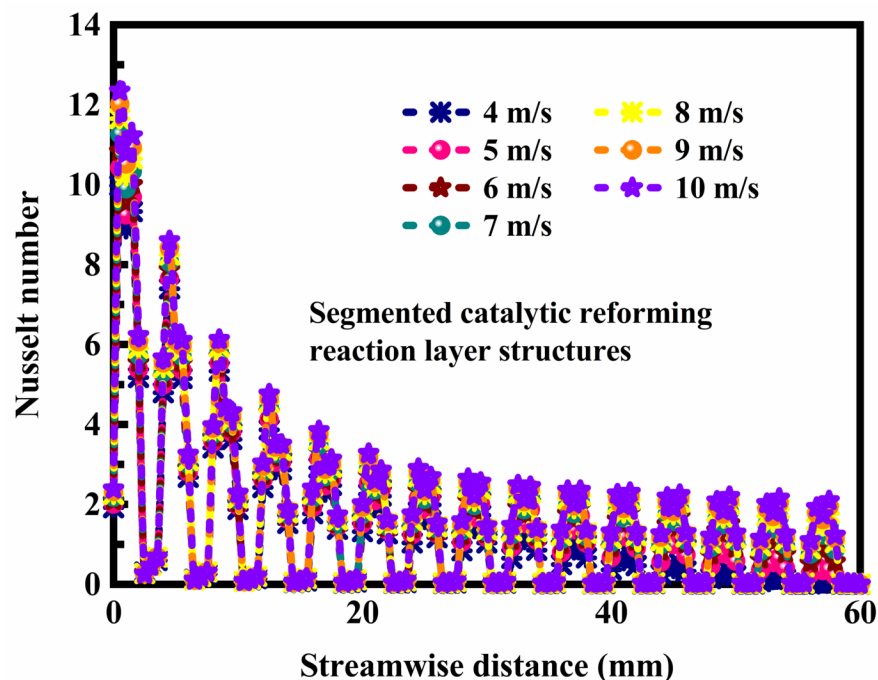


Figure 7. Nusselt number profiles along the length of the thermally integrated reformer with a segmented catalytic reforming reaction layer structure at different velocities of flow at the reactor inlet.

The Nusselt number profiles along the length of the thermally integrated reformer are presented in Figure 8 with different catalytic reaction layer structures. Although the transfer membrane can be provided in a variety of configurations, laminar and tubular membranes are preferred. Laminar membranes are generally employed in pairs which together constitute a membrane envelope, and the requisite zones are preferably provided by furrowing of the membrane surface in a direction transverse to the general direction of flow, although other configurations for the zones may be adopted if so desired. Laminar membranes, when extremely thin, require support for example from a sheet or the like possessing corrugations which define the ridges and furrows in the membrane. It is generally preferable for ridges and furrows in the laminar membranes constituting a membrane envelope to be located opposite each other without significant displacement. The corrugated sheet which may be rigid and formed for example from a plastics material by extrusion, pressing or molding is conveniently provided with substantially planar portions at, or in the region of, two or more edges thereof, the surface of which portions serve to space the ridges in the sheet from those of its neighbor. The latter portions are preferably integral with the sheet. A membrane envelope may be secured between the portions of two adjacent sheets by mechanical pressure applied thereto and preferably with the use of adhesive applied between the envelope and the portions. Adhesive is also preferably applied in the ridges

of the sheet and the membranes. In such cases, the membrane may be furrowed before commencement of fluid flow thereacross but preferably the membrane is planar or only slightly furrowed before introduction of pressurized fluid to the surface thereof which forces the membrane into corrugations in the sheet to form adequate furrows therein. When tubular membranes are employed, which membranes are preferably circular in cross section, the zones are preferably provided by circumferential furrowing. Although the latter configuration for the zones is preferred, others may be employed if so desired. With tubular membranes it may be found particularly convenient to employ a shaped member in the conduit to provide convenient to employ a shaped member in the conduit to provide zones in the region of the membrane surface. The member may for example be a rod or tube possessing circumferential ridges along the length thereof. When in place within the conduit the zones between the ridges are located in the region of the membrane surface and are hence associated therewith.

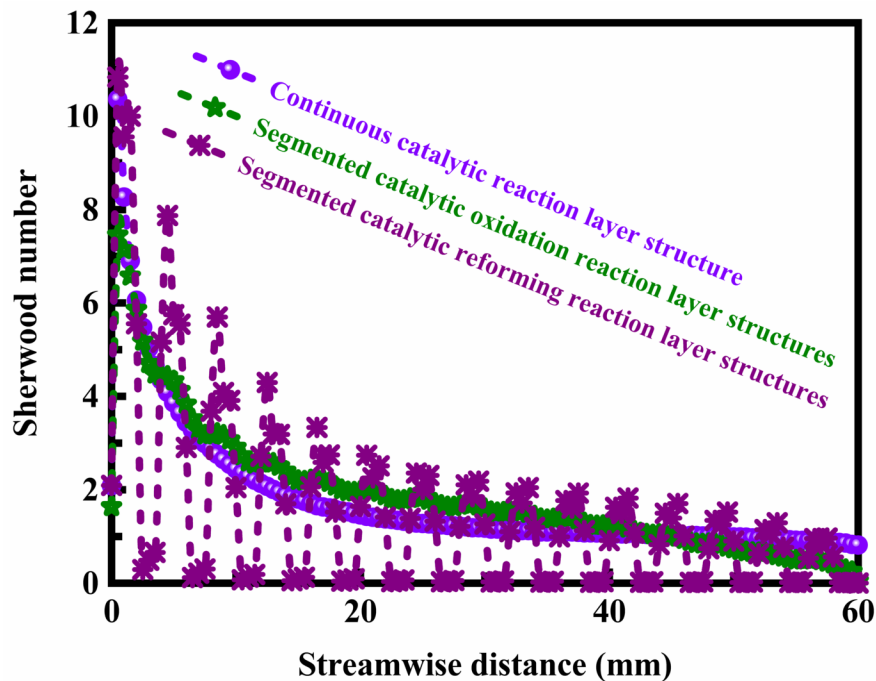


Figure 8. Nusselt number profiles along the length of the thermally integrated reformer with different catalytic reaction layer structures.

4. Conclusions

Numerical simulations are performed using computational fluid dynamics to better understand the characteristics of heat and mass transport in catalytic reaction layers of thermally integrated reformers. The present study aims to provide a fundamental understanding of the heat and mass transport in catalytic reaction layers of thermally integrated reformers. Particular emphasis is placed upon the Sherwood and Nusselt numbers involved in thermally integrated reformer with different catalytic reaction layer structures. The major conclusions are summarized as follows:

- A vapor-liquid equilibrium exists when the escape tendency of the specie from liquid to a vapor phase is exactly balanced with the escape phase at the same temperature and pressure.
- It may be beneficial to utilize the thermodynamic work potential provided by the transfer of heat, whereby the hot input stream is tagged as a heat source and the cold input stream is tagged as a heat sink, to drive the separation process in the desired direction, the entire process occurring in one operation.

- If a chamber partition operates below its maximum heat transfer flux capability, this flux often can be increased by augmenting adjacent latent energy transfer which transfers through the partition as sensible energy.
- The external balance establishes the net enthalpy offset and therefore the temperature difference between the two chambers and the net amount of liquid that may be evaporated or condensed.
- A pure diffusive heat and mass transport would lead to an uneven reaction density or current density in the catalytic reaction layer, on account of a corresponding lack of uniformity in the heat and mass transport in the same catalytic reaction layer.
- A high pressure drop in the thermally integrated reformer is to be avoided, since a high-pressure drop is associated with correspondingly high-power losses, which in turn results in a low overall efficiency.
- The conduit surface may vary along the general direction of flow to provide the zones either intermittently or preferably continuously as with an undulating membrane surface.
- When tubular membranes are employed, which membranes are preferably circular in cross section, the zones are preferably provided by circumferential furrowing.

References

1. G. Athanasaki, A. Jayakumar, and A.M. Kannan. Gas diffusion layers for PEM fuel cells: Materials, properties and manufacturing - A review. *International Journal of Hydrogen Energy* , Volume 48, Issue 6, 2023, Pages 2294-2313.
2. B. Amani and A. Zanj. Analysis of the effects of the gas diffusion layer properties on the effectiveness of baffled flow channels in improving proton exchange membrane fuel cells performance. *International Communications in Heat and Mass Transfer* , Volume 140, 2023, Article Number: 106558.
3. D. Niblett, V. Niasar, S. Holmes, A. Mularczyk, J. Eller, R. Prosser, and M. Mamlouk. Water cluster characteristics of fuel cell gas diffusion layers with artificial microporous layer crack dilation. *Journal of Power Sources* , Volume 555, 2023, Article Number: 232383.
4. W. Yoshimune, S. Kato, M. Inagaki, and S. Yamaguchi. A simple method to measure through-plane effective gas diffusivity of a gas diffusion layer for polymer electrolyte fuel cells. *International Journal of Heat and Mass Transfer* , Volume 191, 2022, Article Number: 122887.
5. A.T. Ertürk, U. Ergin, T. Kadioglu, A.C. Türkmen, and C. Çelik. Metal foams as a gas diffusion layer in direct borohydride fuel cells. *International Journal of Hydrogen Energy* , Volume 47, Issue 55, 2022, Pages 23373-23380.
6. P. Sarkezi-Selsky, H. Schmies, A. Latz, and T. Jahnke. Lattice Boltzmann simulation of liquid water transport in gas diffusion layers of proton exchange membrane fuel cells: Impact of gas diffusion layer and microporous layer degradation on effective transport properties. *Journal of Power Sources* , Volume 556, 2023, Article Number: 232415.
7. J. Sim, M. Kang, and K. Min. Effects of porosity gradient and average pore size in the in-plane direction and disposition of perforations in the gas diffusion layer on the performance of proton exchange membrane fuel cells. *Journal of Power Sources* , Volume 544, 2022, Article Number: 231912.
8. M. Kang, J. Sim, and K. Min. Analysis of surface and interior degradation of gas diffusion layer with accelerated stress tests for polymer electrolyte membrane fuel cell. *International Journal of Hydrogen Energy* , Volume 47, Issue 68, 2022, Pages 29467-29480.
9. G.H. Kim, D. Kim, J. Kim, H. Kim, and T. Park. Impact of cracked gas diffusion layer on performance of polymer electrolyte membrane fuel cells. *Journal of Industrial and Engineering Chemistry* , Volume 91, 2020, Pages 311-316.
10. C. Csoklich, M. Sabharwal, T.J. Schmidt, and F.N. Büchi. Does the thermal conductivity of gas diffusion layer matter in polymer electrolyte fuel cells? *Journal of Power Sources* , Volume 540, 2022, Article Number: 231539.
11. I.S. Lim, Y.I. Lee, B. Kang, J.Y. Park, and M.S. Kim. Electrochemical performance and water management investigation of polymer electrolyte membrane fuel cell (PEMFC) using gas diffusion layer with polytetrafluoroethylene (PTFE) content gradients in through-plane direction. *Electrochimica Acta* , Volume 421, 2022, Article Number: 140509.

12. M. Nasu, H. Yanai, N. Hirayama, H. Adachi, Y. Kakizawa, Y. Shirase, H. Nishiyama, T. Kawamoto, J. Inukai, T. Shinohara, H. Hayashida, and M. Watanabe. Neutron imaging of generated water inside polymer electrolyte fuel cell using newly-developed gas diffusion layer with gas flow channels during power generation. *Journal of Power Sources* , Volume 530, 2022, Article Number: 231251.
13. C. Carral and P. Mele. Modeling the original and cyclic compression behavior of non-woven gas diffusion layers for fuel cells. *International Journal of Hydrogen Energy* , Volume 47, Issue 55, 2022, Pages 23348-23359.
14. H. Pourrahmani and J.V. herle. Water management of the proton exchange membrane fuel cells: Optimizing the effect of microstructural properties on the gas diffusion layer liquid removal. *Energy* , Volume 256, 2022, Article Number: 124712.
15. D. Zapardiel and P.A. García-Salaberri. Modeling the interplay between water capillary transport and species diffusion in gas diffusion layers of proton exchange fuel cells using a hybrid computational fluid dynamics formulation. *Journal of Power Sources* , Volume 520, 2022, Article Number: 230735.
16. M. Sarker, M.A. Rahman, F. Mojica, S. Mehrazi, W.J.M. Kort-Kamp, and P.-Y.A. Chuang. Experimental and computational study of the microporous layer and hydrophobic treatment in the gas diffusion layer of a proton exchange membrane fuel cell. *Journal of Power Sources* , Volume 509, 2021, Article Number: 230350.
17. S. Sakaida, Y. Takahashi, K. Tanaka, and M. Konno. Improvement of polymer electrolyte fuel cell performance by gas diffusion layer with relatively hydrophilic surface. *Journal of Power Sources* , Volume 518, 2022, Article Number: 230730.
18. M. Khatoonabadi, M.A. Safi, N.I. Prasianakis, J. Roth, J. Mantzaras, N. Kirov, and F.N. Büchi. Insights on the interaction of serpentine channels and gas diffusion layer in an operating polymer electrolyte fuel cell: Numerical modeling across scales. *International Journal of Heat and Mass Transfer* , Volume 181, 2021, Article Number: 121859.
19. P. Padavu, P.K. Koorata, and S.D. Bhat. Numerical investigation on the improved reactant mass transport with depth-dependent flow fields in polymer electrolyte fuel cell under inhomogeneous gas diffusion layer compression. *International Journal of Heat and Mass Transfer* , Volume 180, 2021, Article Number: 121796.
20. B.K. Kanchan, P. Randive, and S. Pati. Implications of non-uniform porosity distribution in gas diffusion layer on the performance of a high temperature PEM fuel cell. *International Journal of Hydrogen Energy* , Volume 46, Issue 35, 2021, Pages 18571-18588.
21. S. Cruz-Manzo and P. Greenwood. Low frequency inductive loop in EIS measurements of an open-cathode polymer electrolyte fuel cell stack. Impedance of water vapour diffusion in the cathode catalyst layer. *Journal of Electroanalytical Chemistry* , Volume 900, 2021, Article Number: 115733.
22. A. Alrashidi and H. Liu. Laser-perforated anode gas diffusion layers for direct methanol fuel cells. *International Journal of Hydrogen Energy* , Volume 46, Issue 34, 2021, Pages 17886-17896.
23. W. Yoshimune, S. Kato, and S. Yamaguchi. Multi-scale pore morphologies of a compressed gas diffusion layer for polymer electrolyte fuel cells. *International Journal of Heat and Mass Transfer* , Volume 152, 2020, Article Number: 119537.
24. P.-Y.A. Chuang, M.A. Rahman, F. Mojica, D.S. Hussey, D.L. Jacobson, and J.M. LaManna. The interactive effect of heat and mass transport on water condensation in the gas diffusion layer of a proton exchange membrane fuel cell. *Journal of Power Sources* , Volume 480, 2020, Article Number: 229121.
25. P.A. García-Salaberri. Modeling diffusion and convection in thin porous transport layers using a composite continuum-network model: Application to gas diffusion layers in polymer electrolyte fuel cells. *International Journal of Heat and Mass Transfer* , Volume 167, 2021, Article Number: 120824.
26. S.-H. Lee, J.H. Nam, C.-J. Kim, and H.M. Kim. Effect of fiber orientation on Liquid-Gas flow in the gas diffusion layer of a polymer electrolyte membrane fuel cell. *International Journal of Hydrogen Energy* , Volume 46, Issue 68, 2021, Pages 33957-33968.
27. F. Bezzo, S. Macchietto, and C.C. Pantelides. A general framework for the integration of computational fluid dynamics and process simulation. *Computers & Chemical Engineering* , Volume 24, Issues 2-7,

- 2000, Pages 653-658.
28. A. Brucato, M. Ciofalo, F. Grisafi, and R. Tocco. On the simulation of stirred tank reactors via computational fluid dynamics. *Chemical Engineering Science* , Volume 55, Issue 2, 2000, Pages 291-302.
 29. C.A. Serra, M.R. Wiesner, and J.-M. Lainé. Rotating membrane disk filters: Design evaluation using computational fluid dynamics. *Chemical Engineering Journal* , Volume 72, Issue 1, 1999, Pages 1-17.
 30. M. Bistolfi, N. Mancini, and F. Podenzani. Computational fluid dynamics modelling of multiphase reactors. *Computer Aided Chemical Engineering* , Volume 8, 2000, Pages 379-384.
 31. R. Rieger, C. Weiss, G. Wigley, H.-J. Bart, and R. Marr. Investigating the process of liquid-liquid extraction by means of computational fluid dynamics. *Computers & Chemical Engineering* , Volume 20, Issue 12, 1996, Pages 1467-1475.
 32. C.K. Harris, D. Roekaerts, F.J.J. Rosendal, F.G.J. Buitendijk, P. Daskopoulos, A.J.N. Vreenegeoor, and H. Wang. Computational fluid dynamics for chemical reactor engineering. *Chemical Engineering Science* , Volume 51, Issue 10, 1996, Pages 1569-1594.
 33. R.O. Fox. On the relationship between Lagrangian micromixing models and computational fluid dynamics. *Chemical Engineering and Processing: Process Intensification* , Volume 37, Issue 6, 1998, Pages 521-535.
 34. M. Azaiez, S. Boudoux-Dagonat, M.A. Fikri, and G. Labrosse. The computational fluid dynamics by spectral methods: Some illustrative results. *Computers & Chemical Engineering* , Volume 17, Supplement 1, 1993, Pages S523-S529.
 35. J. Bode. Computational fluid dynamics applications in the chemical industry. *Computers & Chemical Engineering* , Volume 18, Supplement 1, 1994, Pages S247-S251.
 36. A.D. Gosman. Developments in industrial computational fluid dynamics. *Chemical Engineering Research and Design* , Volume 76, Issue 2, 1998, Pages 153-161.
 37. V.M.T.M. Silva and A.E. Rodrigues. Kinetic studies in a batch reactor using ion exchange resin catalysts for oxygenates production: Role of mass transfer mechanisms. *Chemical Engineering Science* , Volume 61, Issue 2, 2006, Pages 316-331.
 38. S. Matthes, T. Merbach, J. Fitschen, M. Hoffmann, and M. Schlüter. Influence of counterdiffusion effects on mass transfer coefficients in stirred tank reactors. *Chemical Engineering Journal Advances* , Volume 8, 2021, Article Number: 100180.
 39. M. Fechtner and A. Kienle. Wave reflections in counter-current separation processes with unequal mass transfer coefficients. *Chemical Engineering Science* , Volume 260, 2022, Article Number: 117929.
 40. J. Guarco, H. Harmuth, and S. Vollmann. Method for determination of mass transfer coefficients for dissolution of dense ceramics in liquid slags. *International Journal of Heat and Mass Transfer* , Volume 186, 2022, Article Number: 122494.
 41. H.N. Vu, X.L. Nguyen, J. Han, and S. Yu. A study on vapor transport characteristics in hollow-fiber membrane humidifier with empirical mass transfer coefficient. *International Journal of Heat and Mass Transfer* , Volume 177, 2021, Article Number: 121549.
 42. E.M. Lakhdiessi, A. Fallahi, C. Guy, and J. Chaouki. Effect of solid particles on the volumetric gas liquid mass transfer coefficient in slurry bubble column reactors. *Chemical Engineering Science* , Volume 227, 2020, Article Number: 115912.
 43. T. Deleau, M.H.H. Fechter, J.-J. Letourneau, S. Camy, J. Aubin, A.S. Braeuer, and F. Espitalier. Determination of mass transfer coefficients in high-pressure two-phase flows in capillaries using Raman spectroscopy. *Chemical Engineering Science* , Volume 228, 2020, Article Number: 115960.
 44. K.C. Sandeep, S. Mohan, D. Mandal, and S. Mahajani. Determination of gas film mass transfer coefficient in a packed bed reactor for the catalytic combustion of hydrogen. *Chemical Engineering Science* , Volume 202, 2019, Pages 508-518.
 45. M. Fechtner and A. Kienle. Approximate shock layer solutions for the separation of multicomponent mixtures with different axial dispersion or mass transfer coefficients. *Chemical Engineering Science* , Volume 231, 2021, Article Number: 116335.
 46. A.D. Pérez, B.V.D. Bruggen, and J. Fontalvo. Study of overall mass transfer coefficients in a liquid

membrane in Taylor flow regime: Calculation and correlation. *Chemical Engineering and Processing - Process Intensification* , Volume 134, 2018, Pages 20-27.

47. K. Scott, W.M. Taama, P. Argyropoulos, and K. Sundmacher. The impact of mass transport and methanol crossover on the direct methanol fuel cell. *Journal of Power Sources* , Volume 83, Issues 1-2, 1999, Pages 204-216.
48. M. Wöhr, K. Bolwin, W. Schnurnberger, M. Fischer, W. Neubrand, and G. Eigenberger. Dynamic modelling and simulation of a polymer membrane fuel cell including mass transport limitation. *International Journal of Hydrogen Energy* , Volume 23, Issue 3, 1998, Pages 213-218.
49. D. Singh, D.M. Lu, and N. Djilali. A two-dimensional analysis of mass transport in proton exchange membrane fuel cells. *International Journal of Engineering Science* , Volume 37, Issue 4, 1999, Pages 431-452.
50. K. Scott, W.M. Taama, S. Kramer, P. Argyropoulos, and K. Sundmacher. Limiting current behaviour of the direct methanol fuel cell. *Electrochimica Acta* , Volume 45, Issue 6, 1999, Pages 945-957.
51. A. Khalidi, B. Lafage, P. Taxil, G. Gave, M.J. Clifton, and P. Cézac. Electrolyte and water transfer through the porous electrodes of an immobilised-alkali hydrogen-oxygen fuel cell. *International Journal of Hydrogen Energy* , Volume 21, Issue 1, 1996, Pages 25-31.
52. K. Scott, P. Argyropoulos, and K. Sundmacher. A model for the liquid feed direct methanol fuel cell. *Journal of Electroanalytical Chemistry* , Volume 477, Issue 2, 1999, Pages 97-110.
53. D. Chu and R. Jiang. Comparative studies of polymer electrolyte membrane fuel cell stack and single cell. *Journal of Power Sources* , Volume 80, Issues 1-2, 1999, Pages 226-234.
54. A.S. Aricò, P. Cretì, V. Baglio, E. Modica, and V. Antonucci. Influence of flow field design on the performance of a direct methanol fuel cell. *Journal of Power Sources* , Volume 91, Issue 2, 2000, Pages 202-209.
55. H. Dohle, J. Divisek, and R. Jung. Process engineering of the direct methanol fuel cell. *Journal of Power Sources* , Volume 86, Issues 1-2, 2000, Pages 469-477.
56. J. Cunha and J.L.T. Azevedo. Modelling the integration of a compact plate steam reformer in a fuel cell system. *Journal of Power Sources* , Volume 86, Issues 1-2, 2000, Pages 515-522.
57. D. Benavente, M.A.G.D. Cura, R. Fort, and S. Ordóñez. Thermodynamic modelling of changes induced by salt pressure crystallisation in porous media of stone. *Journal of Crystal Growth* , Volume 204, Issues 1-2, 1999, Pages 168-178.
58. M. Awartani and M.H. Hamdan. Non-reactive gas-particulate models of flow through porous media. *Applied Mathematics and Computation* , Volume 100, Issue 1, 1999, Pages 93-102.
59. J. Bergendahl and D. Grasso. Prediction of colloid detachment in a model porous media: Hydrodynamics. *Chemical Engineering Science* , Volume 55, Issue 9, 2000, Pages 1523-1532.
60. Q.S. Chen, V. Prasad, A. Chatterjee, and J. Larkin. A porous media-based transport model for hydrothermal growth. *Journal of Crystal Growth* , Volumes 198-199, Part 1, 1999, Pages 710-715.
61. T. Masuoka and Y. Takatsu. Turbulence model for flow through porous media. *International Journal of Heat and Mass Transfer* , Volume 39, Issue 13, 1996, Pages 2803-2809.
62. X. Lu, P. Xie, D.B. Ingham, L. Ma, and M. Pourkashanian. A porous media model for CFD simulations of gas-liquid two-phase flow in rotating packed beds. *Chemical Engineering Science* , Volume 189, 2018, Pages 123-134.
63. T. Santagata, R. Solimene, G. Aprea, and P. Salatino. Modelling and experimental characterization of unsaturated flow in absorbent and swelling porous media. *Chemical Engineering Science* , Volume 224, 2020, Article Number: 115765.
64. P. Gurikov, A. Kolnoochenko, M. Golubchikov, N. Menshutina, and I. Smirnova. A synchronous cellular automaton model of mass transport in porous media. *Computers & Chemical Engineering* , Volume 84, 2016, Pages 446-457.
65. M. Veyskarami, A.H. Hassani, and M.H. Ghazanfari. Modeling of non-Darcy flow through anisotropic porous media: Role of pore space profiles. *Chemical Engineering Science* , Volume 151, 2016, Pages 93-104.
66. B.R. Becker and B.A. Fricke. Modeling transport processes in heat and mass releasing porous media.

Characteristics analysis of heat and mass transport in catalytic reaction layers of thermally integrated reformers

Junjie Chen

Department of Energy and Power Engineering, School of Mechanical and Power Engineering, Henan Polytechnic University, Jiaozuo, Henan, 454000, P.R. China

* Corresponding author, E-mail address: cjjtpj@163.com, <https://orcid.org/0000-0002-4222-1798>

Abstract

In conventional fuel cells, a predominantly diffusive heat and mass transport is established in the diffusion layer. However, conventional fuel cells cannot ensure a heat and mass transport from the porous diffusion layer to the catalytic reaction layer that is sufficiently uniform for this purpose. The present study aims to provide a methodology for determining the characteristics of heat and mass transport in catalytic reaction layers. Numerical simulations are performed using computational fluid dynamics to better understand the characteristics of heat and mass transport in catalytic reaction layers of thermally integrated reformers. The present study aims to provide a fundamental understanding of the heat and mass transport in catalytic reaction layers of thermally integrated reformers. Particular emphasis is placed upon the dimensionless quantities involved in thermally integrated reformer with different catalytic reaction layer structures. The results indicate that a vapor-liquid equilibrium exists when the escape tendency of the specie from liquid to a vapor phase is exactly balanced with the escape phase at the same temperature and pressure. It may be beneficial to utilize the thermodynamic work potential provided by the transfer of heat to drive the separation process in the desired direction. If a chamber partition operates below its maximum heat transfer flux capability, this flux often can be increased by augmenting adjacent latent energy transfer which transfers through the partition as sensible energy. The external balance establishes the net enthalpy offset and therefore the temperature difference and the net amount of liquid that may be evaporated or condensed. A pure diffusive heat and mass transport would lead to an uneven reaction density or current density in the catalytic reaction layer, on account of a corresponding lack of uniformity in the heat and mass transport in the same catalytic reaction layer. A high pressure-drop in the thermally integrated reformer is to be avoided, since a high-pressure drop is associated with correspondingly high-power losses, which in turn results in a low overall efficiency. The conduit surface may vary along the general direction of flow to provide the zones either intermittently or preferably continuously as with an undulating membrane surface. When tubular membranes are employed, which membranes are preferably circular in cross section, the zones are preferably provided by circumferential furrowing.

Keywords: Integrated reformers; Temperature differences; Membrane surfaces; Dimensionless quantities; Heat transport; Mass transport

1. Introduction

It is of great importance to improve a heat and mass transport in a diffusion layer of a fuel cell [1, 2]. The diffusion layer is connected to a bipolar element which has a plurality of channels for carrying an operating medium [3, 4]. Fuel cells having a diffusion layer and methods of operating such fuel cells are generally known [5, 6]. The operating principle of a fuel cell is based on the principle that in an electro-chemical reaction, namely reactants such as hydrogen and oxygen react to form products such as water [7, 8]. The electrochemical reaction produces a potential difference and an electric current, so that

electrical energy can be generated directly by the fuel cell.

A fuel cell includes two catalytic reaction layers which are spaced apart from one another and have a membrane disposed between them [9, 10]. In this case, an anode reaction takes place in one reaction layer and a cathode reaction takes place in the other reaction layer [11, 12]. The membrane ensures a desired transport of charge carriers, for example of protons. Both catalytic reaction layers are operatively connected to in each case one porous diffusion layer, in such a manner that reactants, such as hydrogen and oxygen, and reaction products, for example, water, of the electro-chemical reaction as well as electrons are fed to or removed from the corresponding catalytic reaction layer [13, 14]. In the porous diffusion layer, gas is transported through the pores thereof, while at the same time electrons are transported through the electrically conductive structure of the same diffusion layer [15, 16]. The porous diffusion layer is connected to a bipolar plate or a bipolar element, which on its contact side is provided with channels for carrying an operating medium, which are open at the edges, and webs correspondingly disposed between the channels.

The flow channels in the bipolar plate are used to transport, namely remove or supply, gaseous reactants, namely the starting material or operating medium, and reaction products, while the webs are used in a corresponding manner to supply and remove electrons [17, 18]. In conventional fuel cells, a predominantly diffusive heat and mass transport is established in the diffusion layer [19, 20]. The upper power range of a fuel cell, high current density, is limited by the mass transport of reactants or reaction products through the diffusion layer to or from the catalytic reaction layer and by the transport of waste heat from the catalytic reaction layer through the diffusion layer [21, 22]. In principle, it is desirable to have a heat and mass transport between the porous diffusion layer and the adjoining catalytic reaction layer that is as uniform as possible [23, 24], in order to achieve a correspondingly uniform reaction density or current density in the same catalytic reaction layer [25, 26]. Conventional fuel cells cannot ensure a heat and mass transport from the porous diffusion layer to the catalytic reaction layer that is sufficiently uniform for this purpose.

The present study is focused primarily upon the characteristics analysis of heat and mass transport in catalytic reaction layers of thermally integrated reformers. Numerical simulations are performed using computational fluid dynamics to better understand the heat and mass transport characteristics. Heat transport, any or all of several kinds of phenomena, is considered as mechanisms, that convey energy and entropy from one location to another. The specific mechanisms are usually referred to as convection, thermal radiation, and conduction. Conduction involves transfer of energy and entropy between adjacent molecules, usually a slow process. Convection involves movement of a heated fluid, usually a fairly rapid process. Radiation refers to the transmission of energy as electromagnetic radiation from its emission at a heated surface to its absorption on another surface. In physics, transport phenomenon is any of the phenomena involving the movement of various entities, such as mass, momentum, or energy, through a medium, fluid or solid, by virtue of nonuniform conditions existing within the medium. Variations of concentration in a medium, for example, lead to the relative motion of the various chemical species present, and this mass transport is generally referred to as diffusion. Variations of velocity within a fluid result in the transport of momentum, which is normally referred to as viscous flow. Variations in temperature result in the transport of energy, a process usually called heat conduction. There are many similarities in the mathematical descriptions of these three phenomena, and the three often occur together physically, as in combustion, where a flowing viscous fluid mixture is undergoing chemical reactions that produce heat, which is conducted away, and that produce various chemical species that inter-diffuse with one another. The present study aims to provide a fundamental understanding of the heat and mass transport in catalytic reaction layers of thermally integrated reformers. Particular emphasis is placed upon the Sherwood and Nusselt numbers involved in thermally integrated reformer with different catalytic reaction layer structures.

2. Methods

Computational fluid dynamics is a common approach for improving the understanding of hydrodynamics, thermodynamics, and chemical kinetics of a flow system [27, 28]. Computational fluid dynamics codes have been evolving over the past two decades [29, 30] with great advances in both the numerical techniques and computer hardware [31, 32]. Computational fluid dynamics applications have been extended from simple laboratory-type problems to complex industrial-type flow systems [33, 34]. Computer simulation has gained widespread acceptance as an effective and cost-saving tool to further improve the performance of flow systems [35, 36]. The present study aims to provide a methodology for determining local kinetic model constants using local fluid dynamic effects in the analysis of chemical flow reactor systems and to extract local chemical kinetic model constants in a reacting flow computational fluid dynamics computer code for a reaction set and reactor system for optimizing system operating parameters and design. The present study also aims to provide an analysis approach which couples computational fluid dynamics with kinetic computations to provide local kinetic constants useful over a broad range of operating conditions for specific and complex reaction sets in specific and complex reactor systems.

The present study contemplates a methodology to extract local chemical kinetic model constants for use in a reacting flow computational fluid dynamics computer code coupled with chemical kinetic computations. Obtaining local kinetic model constants as opposed to global model constants is necessary for computing reaction and product yields in non-uniform flow fields under a broad range of operating conditions for a chemical reactor system. A key feature of the methodology is that it uses the coupled computational fluid dynamics and kinetic computer code in combination with data obtained from a matrix of experimental tests to extract the kinetic constants. This approach implicitly includes the local fluid dynamic effects in the extracted local kinetic constants for each particular application system to which the methodology is applied. The application of the methodology does not produce a universal set of kinetic model constants for a specified set of chemical reactions that will work well in computations for systems that are greatly different in geometry or other significant characteristics. No known method for producing such a set of constants exists, except for very simple reaction sets limited also to relatively simple reactor systems. The present methodology provides a means to extract local kinetic model constants that work well over a fairly broad range of operating conditions for specific and complex reaction sets in specific and complex reactor systems. Once the kinetic model constants are extracted for a reaction set and reactor system, the model constants can be used in the coupled computational fluid dynamics and chemical kinetic code to optimize the operating conditions or design of the system, including planned retrofit design improvements to existing systems.

The local kinetic model constant extraction methodology requires the use of a computational scheme for coupling computational fluid dynamics calculations with chemical kinetic calculations in a novel two stage approach that avoids numerical stiffness problems that frequently arise when computational fluid dynamics and chemical kinetic computations are coupled. The computer code in which this two-stage approach is implemented and used to test the methodology is a computational fluid dynamics program. Boundary conditions consist of flow inlets and exit boundaries, wall, repeating, and pole boundaries, and internal face boundaries. Velocity inlet boundary conditions are used to define the velocity and scalar properties of the flow at inlet boundaries. Pressure inlet boundary conditions are used to define the total pressure and other scalar quantities at flow inlets. Mass flow inlet boundary conditions are used in compressible flows to prescribe a mass flow rate at an inlet. It is not necessary to use mass flow inlets in incompressible flows because when density is constant, velocity inlet boundary conditions will fix the mass flow. Like pressure and velocity inlets, other inlet scalars are also prescribed. Pressure outlet boundary conditions are used to define the static pressure at flow outlets and also other scalar variables,

in case of backflow. The use of a pressure outlet boundary condition instead of an outflow condition often results in a better rate of convergence when backflow occurs during iteration.

Pressure far-field boundary conditions are used to model a free-stream compressible flow at infinity, with free-stream Mach number and static conditions specified. This boundary type is available only for compressible flows. Outflow boundary conditions are used to model flow exits where the details of the flow velocity and pressure are not known prior to solution of the flow problem. They are appropriate where the exit flow is close to a fully developed condition, as the outflow boundary condition assumes a zero streamwise gradient for all flow variables except pressure. They are not appropriate for compressible flow calculations. Inlet vent boundary conditions are used to model an inlet vent with a specified loss coefficient, flow direction, and ambient or inlet total pressure and temperature. Intake fan boundary conditions are used to model an external intake fan with a specified pressure jump, flow direction, and ambient or intake total pressure and temperature. Outlet vent boundary conditions are used to model an outlet vent with a specified loss coefficient and ambient or discharge static pressure and temperature. Exhaust fan boundary conditions are used to model an external exhaust fan with a specified pressure jump and ambient or discharge static pressure. Wall boundary conditions are used to bound fluid and solid regions. In viscous flows, the no-slip boundary condition is enforced at walls by default, but you can specify a tangential velocity component in terms of the translational or rotational motion of the wall boundary, or model a slip wall by specifying shear.

3. Results and discussion

The Sherwood number profiles along the length of the thermally integrated reformer with a continuous catalytic reaction layer structure are presented in Figure 1 at different velocities of flow at the reactor inlet. Dimensional consistency is required when computing formulas using dimensional quantities. For example, when adding two dimensional quantities together, both dimensional quantities must represent the same kind of dimensional measurement. Dimensional consistency requires knowing not just the units of measure used for the input dimensional quantities, but also the kind of measurement each unit refers to. Through the use of a gas which is generally defined as a noncondensing vapor or gas and in most cases is ambient air. This gas generally flows through a chamber which is thermally connected to a heat sink and in one case a heat source. Thermally connected, in this context, means that fluids from a chamber are brought into close proximity of a heat transferring barrier so that heat can transfer from a chamber to a sink or from a source to a chamber. In its passage, the gas generally operates under nearly constant pressure with pressure changed caused by frictional losses. The heat sources and sinks being of different temperature than the gas in the chamber cause a temperature and absolute humidity change to be created in the gas from one end of the chamber to the other. These changes cause the gases to approach a vapor-liquid equilibrium value and be thus receptive to receiving or losing vapors. Equilibrium value is a vapor-liquid equilibrium concentration or temperature. A vapor-liquid equilibrium exists when the escape tendency of the specie from liquid to a vapor phase is exactly balanced with the escape phase at the same temperature and pressure. In operation, where there is evaporation from the wetting desiccant into the gas stream or selective condensation from this gas stream, segmented wetting coupled with migratory movement provide the following occurrences. First, as a sector is wetted by primarily the same wetting desiccant, the now localized wetting desiccant temperature and composition can be forced to change. Second, as the migratory movement is from one sector to another, the concentration of one sector influences the wetting desiccant composition of the subsequent sector where it again may be altered by evaporation or condensation. In this manner, selected desiccant property gradients can be developed and maintained throughout the chamber length. The apparatus consists of a chamber and heat sink which generally is found throughout the chamber length. A gas is moved into the chamber by mechanical means which can be a low-pressure blower. Multiple liquid segmentations

generally caused by segregated pumping and distribution means are provided. This distribution generally encompasses wetting of the heat sink barrier, but may further include wetting methods to increase chamber gas and wetting desiccant contact area, for example, the use of droplet sprays. The number of segmentations is sufficient to allow the wetting desiccant temperature to approach the temperatures of the passing gas proximate thereto and also present any significant concentration variances developed within the wetting desiccant.

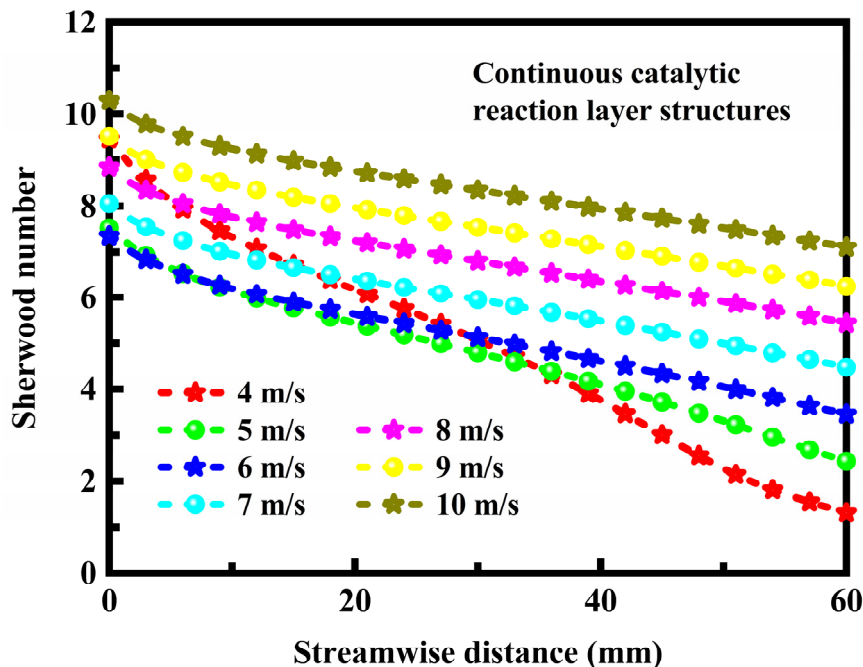


Figure 1. Sherwood number profiles along the length of the thermally integrated reformer with a continuous catalytic reaction layer structure at different velocities of flow at the reactor inlet.

The Sherwood number profiles along the length of the thermally integrated reformer with a segmented catalytic oxidation reaction layer structure are presented in Figure 2 at different velocities of flow at the reactor inlet. Mass exchange between two phases is of particular importance largely because it is involved in most separation processes, as for example in the recovery of a pure product from a mixture [37, 38]. Most practical schemes are based on the fact that concentrations of two phases in equilibrium with each other are quite different [39, 40]. Any method of contacting two phases which results in the selective interphase transport of one of the constituents can form the basis of a separation process [41, 42]. The selectivity can be the result of different equilibrium composition for the different species or it may be due to different rates of transport of the several constituents [43, 44]. Thermodynamic work potential of several kinds may serve to implement mass exchange. In electrochemical processes, an electrical potential provides the motive force, while in a column for the separation of gaseous isotopes, it is a thermal gradient [45, 46]. However, in the majority of applications in the process industries, it is the concentration gradient which provides the driving force to effect mass exchange between two phases. This is a well-established operation carried generally in a multi-stage operation such as in distillation towers, mixer-settler units, and is based on well-known theory. Thermodynamic considerations require that work be invested in a system in order for its components to be separated, involving a decrease in entropy. Heat transfer between a relatively hot body and a relatively cold body is also a well-established unit operation that is carried in a variety of devices such as heat exchangers and heat regenerators. It may be beneficial to utilize the thermodynamic work potential provided by the transfer of heat, whereby the hot input stream is tagged as a heat source and the cold input stream is tagged as a heat sink, to drive the separation process in the desired direction, the entire process occurring in one operation. This integration may be beneficial both from the point view of energy utilization and by virtue of the compactness of the

equipment which would perform two functions simultaneously, for example, in catalytic reaction layers of thermally integrated reformers. The overall efficiency of the process will depend on a number of factors such as: the amount and adsorbing power of the adsorbing reagent as a function of temperature; the heat capacities of the adsorbing reagent and of the fluids; flow rates, temperatures and compositions of the inlet streams and the thermodynamical properties of the materials involved.

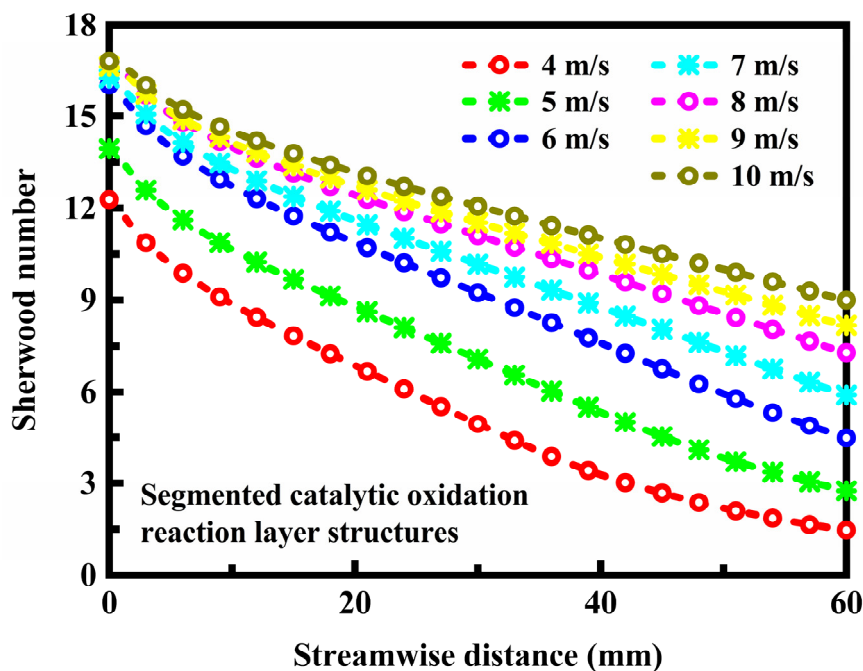


Figure 2. Sherwood number profiles along the length of the thermally integrated reformer with a segmented catalytic oxidation reaction layer structure at different velocities of flow at the reactor inlet.

The Sherwood number profiles along the length of the thermally integrated reformer with a segmented catalytic reforming reaction layer structure are presented in Figure 3 at different velocities of flow at the reactor inlet. The design can be presented in terms of heat transfer and mass and energy balances. The conduction of energies between chambers always involves sensible heat and, generally, at least one latent heat transfer related to evaporation or condensation. Sensible heat is that heat required to change the temperature of a substance without changing the state of the substance. Latent heat is that heat required to change the state of the substance from solid to liquid or from liquid to gas without change of temperature or pressure. A basic heat transfer is established by the auxiliary heat exchange to the gas before this gas returns to the second chamber. This exchange causes a temperature differential between the gas in each chamber. In order to preserve this temperature differential along the chamber lengths, the gases are made to flow in a thermally counter-current direction in the first and second chambers. This thermally counter-current gas movement results from the thermal connection between the sequentially ordered sectors of the first and second chambers by means of the heat transferring partitions. The continually changing temperatures of the gas within the chambers cause a continual shifting of the vapor-liquid equilibrium value between the liquid and gas phases. This shifting allows evaporation and condensation between the moving gas and the wetting substances. The energies released in condensation are normally transferred to the other chamber allowing for additional evaporation to occur from the wetting substances. Where many sectors are wetted, as in the case of the concentration and fractionation modes, these transfers of latent energy are many times the sensible energy related to the temperature change of the gas. This sensible exchange, in turn, is greater than any auxiliary heat exchange into the gas. In other operating modes, the latent energies associated with evaporation from the segmented wetting substances can be turned to sensible energies in that such evaporation can cause the gas to further lower in temperature. Generally speaking, minimum wetting substance movement occurs when energy transfer

between chambers involves exchange directly through wetted partitions separating the chambers. However, there are occasions when this minimum is balanced against other rates. One concern is the rate of energy conducting through a certain partition area including liquids on the partition, called the partition heat transfer flux. The partition heat transfer flux is maximized if the temperature difference across the partition is increased to a maximum value of the specified temperature differential between chambers. If a chamber partition operates below its maximum heat transfer flux capability, this flux often can be increased by augmenting adjacent latent energy transfer which transfers through the partition as sensible energy. This augmentation involves inclusion of additional gas-liquid heat transfer contact area beyond that supplied by wetting the partition, for example, by the use of spray droplets within the chamber area. This expansion of latent transfer surface is useful. Conversely, in other cases such as some concentration operations, latent transfer within the chambers is capable of being in excess of the maximum partition flux. When both chambers are segmented wetted, an increased partition area can be supplied by thermally connected partitions that are external to the chambers. In this manner, the partition heat transfer flux can operate at its maximum along with increased chamber sensible and latent heat transfer.

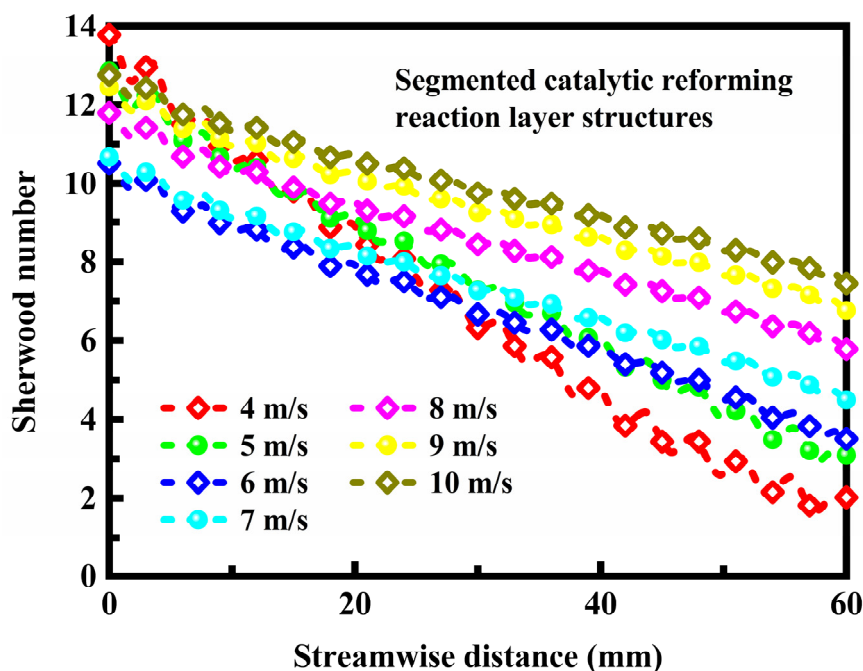


Figure 3. Sherwood number profiles along the length of the thermally integrated reformer with a segmented catalytic reforming reaction layer structure at different velocities of flow at the reactor inlet.

The Sherwood number profiles along the length of the thermally integrated reformer are presented in Figure 4 with different catalytic reaction layer structures. A net overall mass and energy balance encompassing the entire process includes the enthalpy of the incoming gas plus the input energy to this gas from an auxiliary heat exchange all being equal to the enthalpy of the exiting gas. In some modes of operation, there is also the enthalpy of a feed material and the enthalpy of a product material, as for example in concentration which may involve an incoming brackish water and products of substantially pure water and brine concentrate. The energy associated with these feeds and products tends to either cancel or be made inconsequential. The above energy balance reveals that where both gas streams are saturated and the auxiliary heat exchange adds energy, for example in the concentration and fractionation modes, there would be a shift in temperature of those gas streams in the same direction as the shift in enthalpies. In this way the gas stream with the highest enthalpy and highest temperature would be associated with the cooling or condensing chamber allowing its energy to be transmitted to the lower enthalpy and lower temperature gas stream located in the heating or evaporation chamber and thereby reused. Owing to the differences in saturation, there can be a shift in temperature of those gas streams in

the opposite direction as the shift in enthalpies. The gas stream with the lowest enthalpy but highest temperature would be associated with the cooling chamber allowing its energy to be transmitted to the higher enthalpy but lower temperature gas stream located in the second chamber. In summary, the external balance establishes the net enthalpy offset and therefore the temperature difference between the two chambers and the net amount of liquid that may be evaporated or condensed. An internal chamber energy balance gives detail on the actual amount of temperature rise or fall in a chamber and on the actual amount of liquid evaporated or condensed in a chamber. An internal mass and energy balance around a chamber equates the incoming gas enthalpy to a chamber plus the conducting energies associated with the partition to the exiting gas enthalpy from a chamber. The two forms of conducting energies are sensible energy needed to heat up or cool down chamber gas, and latent energy needed for evaporation or condensation into or out of the chamber gas. The internal chamber balance also relates the chamber exiting gas temperatures to the amount of sensible and latent energies that can transfer to the gas in a chamber. The more energies that can transmit to the chamber gas the larger will be the temperature rise and fall and actual evaporation into or actual condensation out of the chamber gas from the chamber entrance to chamber exit.

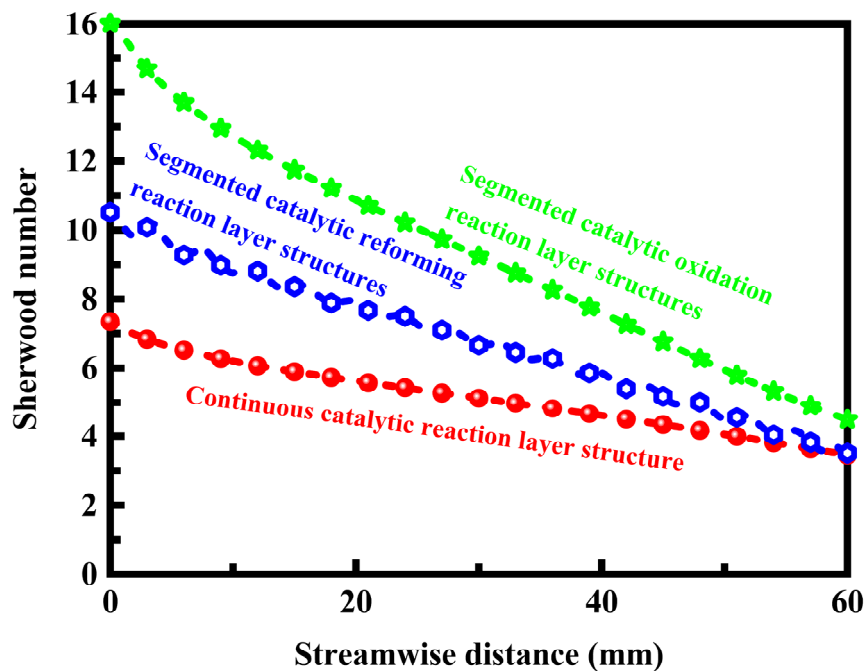


Figure 4. Sherwood number profiles along the length of the thermally integrated reformer with different catalytic reaction layer structures.

The Nusselt number profiles along the length of the thermally integrated reformer with a continuous catalytic reaction layer structure are presented in Figure 5 at different velocities of flow at the reactor inlet. The diffusion layer is connected to a bipolar element which includes a plurality of channels for carrying an operating medium. The heat and mass transport in a diffusion layer is characterized in that a pressure difference is generated in at least two adjacent channels for carrying operating medium, so as to form a convective heat and mass transport. A pressure difference is generated in at least two adjacent channels for carrying an operating medium, so as to form a convective heat and mass transport. In this context, a distinction needs to be drawn between a diffusive and a convective heat and mass transport. A diffusive transport is established on account of the existence of a concentration gradient or a temperature gradient, while a convective transport is attributable to the presence of a pressure gradient. Therefore, both a diffusive heat and mass transport and a corresponding convective heat and mass transport are produced, since there is a sufficiently great pressure gradient between at least two adjacent channels for carrying an operating medium. A pure diffusive heat and mass transport would lead to an uneven reaction

density or current density in the catalytic reaction layer, on account of a corresponding lack of uniformity in the heat and mass transport in the same catalytic reaction layer. A reaction density or current density which is more uniform compared to the previous designs can be achieved in the catalytic reaction layer by the convective heat and mass transport which is additionally established in accordance with the design. In this context, the term adjacent channels for carrying an operating medium can also be understood as meaning corresponding channel sections that are adjacent to one another.

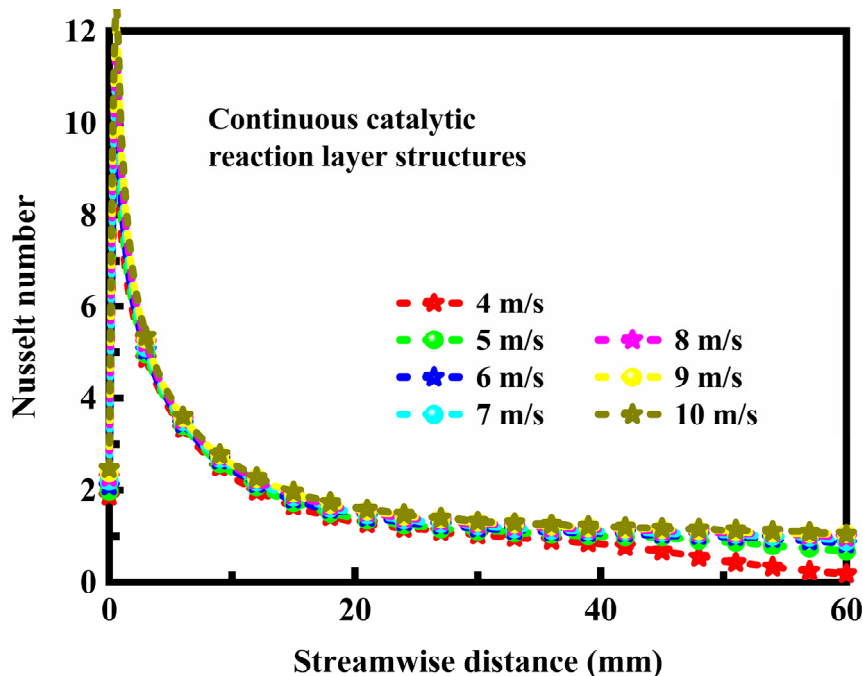


Figure 5. Nusselt number profiles along the length of the thermally integrated reformer with a continuous catalytic reaction layer structure at different velocities of flow at the reactor inlet.

The Nusselt number profiles along the length of the thermally integrated reformer with a segmented catalytic oxidation reaction layer structure are presented in Figure 6 at different velocities of flow at the reactor inlet. The operating medium advantageously includes gaseous reaction products and gaseous reactants or reaction starting materials. The reaction products may be water and the reaction starting materials or reactants may be hydrogen and oxygen, which are each carried through the channels for carrying an operating medium in the gaseous state. Accordingly, hydrogen and oxygen are transported as reactants in the diffusion layer. The substances which are to be transported in the diffusion layer are preferably reactants, in particular hydrogen and oxygen, reaction products, in particular water, and electrons [47, 48]. The use of these substances in a fuel cell is already known [49, 50]. These substances are transported from the diffusion layer to a catalytic reaction layer of the thermally integrated reformer. The gaseous reactants are supplied as pure reactants or as part of a mixture [51, 52]. The bipolar element is preferably configured as a surface-structured bipolar plate with, on one surface, channels for carrying an operating medium, which are open at the edges, and webs disposed between them. The channels for carrying the operating medium are used to supply and remove the gaseous reactants and reaction products, while electrons are correspondingly supplied and removed via the webs. Gaseous reaction products and reaction starting materials, and also electrons, pass into the diffusion layer [53, 54]. In other words, the surface-structured bipolar plate has a surface formed with webs between the channels, which are open at the surface of the bipolar plate [55, 56]. The pressure difference is generated in each case in two adjacent channels for carrying the operating medium and, at the same time, the pressure drop between an operating-medium inlet and an operating-medium outlet of the thermally integrated reformer is minimized. A high pressure drop in the thermally integrated reformer is to be avoided, since a high-pressure drop is associated with correspondingly high-power losses for example in compressors which

in turn results in a low overall efficiency. Therefore, a pressure difference between two adjacent channels for carrying an operating medium is particularly desirable, however, at the same time, a low pressure drop with regard to the thermally integrated reformer as a whole should be provided.

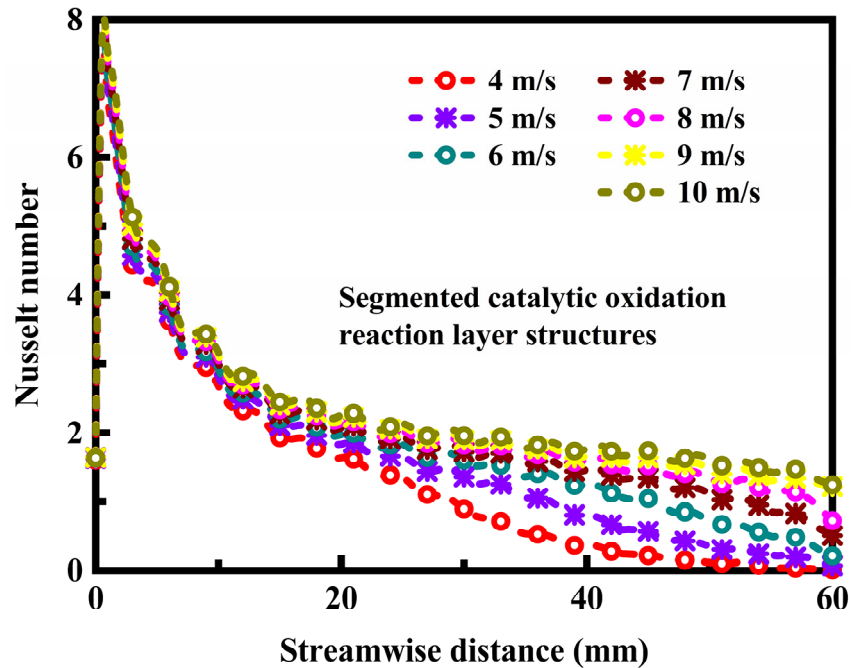


Figure 6. Nusselt number profiles along the length of the thermally integrated reformer with a segmented catalytic oxidation reaction layer structure at different velocities of flow at the reactor inlet.

The Nusselt number profiles along the length of the thermally integrated reformer with a segmented catalytic reforming reaction layer structure are presented in Figure 7 at different velocities of flow at the reactor inlet. Macroscopic description of porous media is based on two basic assumptions: continuous medium approximation, which disregards microscopic structure of the material and assumes continuous distribution of the matter in space, and phenomenological response coefficient approximation, which disregards internal degrees of freedom of the material and assumes that the material responds to the external force, such as temperature or pressure gradient and electric potential, as an unstructured entity with certain response coefficient, such as thermal conductivity, permeability, and electric conductivity [57, 58]. Since macroscopic modeling is a primary tool in many industrial and scientific applications, the microscopic modeling is often considered an auxiliary tool for estimating the macroscopic response coefficients [59, 60]. However, the macroscopic models are insufficient. One-phase macroscopic fluid transport model is based on permeability coefficient [61, 62]. It is well known, that a rather extensive set of one-phase transport phenomena lies outside the permeability coefficient concept [63, 64]. Multiphase fluid transport model is based on phase permeability coefficients, and this approach is insufficient and microscopic processes are important [65, 66]. The conduit configuration varies periodically along the general direction of flow, either inherently or in response to fluid pressure therein, in order to give rise to separation and reattachment of the flow at a multiplicity of zones within the conduit whereby secondary flow is induced within the zones. The zones which can vary considerably in configuration are generally spaced one from another by constrictions to flow through the conduit. When fluid is pulsated across a constriction, the flow is detached therefrom and re-attaches at a neighboring constriction with eddy formation in the zone between the constrictions. The eddies which reduce the boundary layer effect generally take the form of vortices, the axes of which are transverse to the general direction of flow. The conduit surface, typically the surface of the membrane, may vary along the general direction of flow to provide the zones either intermittently or preferably continuously as with an undulating membrane surface. The zones may take a variety of configurations. In particular, they may extend across the surface

of the conduit transverse to the direction of flow to provide furrows or may be present as local depressions such as dimples in a conduit surface, such depressions preferably having curved bases and conveniently being hemispherical. When the surface of the membrane is shaped into zones in response to the pressure of fluid in the conduit, one or more means are provided associated with the membrane for constraining the latter to adopt the required configuration in response to the pressure of fluid therein. However, zones may be provided in the region of the membrane surface by a shaped member within the conduit and conveniently formed prior to insertion therein. The membrane itself is conveniently tubular and the means for constraining the fluid flow in a helical path may be formed by twisting a strip of material about its longitudinal axis to provide an insert which preferably fits tightly inside the tube. When fluid in pulsated in the conduit, secondary rotary flow is induced in the fluid the axis of which lies generally in the direction of flow. Such secondary flow enhances the mixing action promoted by the helical fluid motion and facilitates transfer through the membrane.

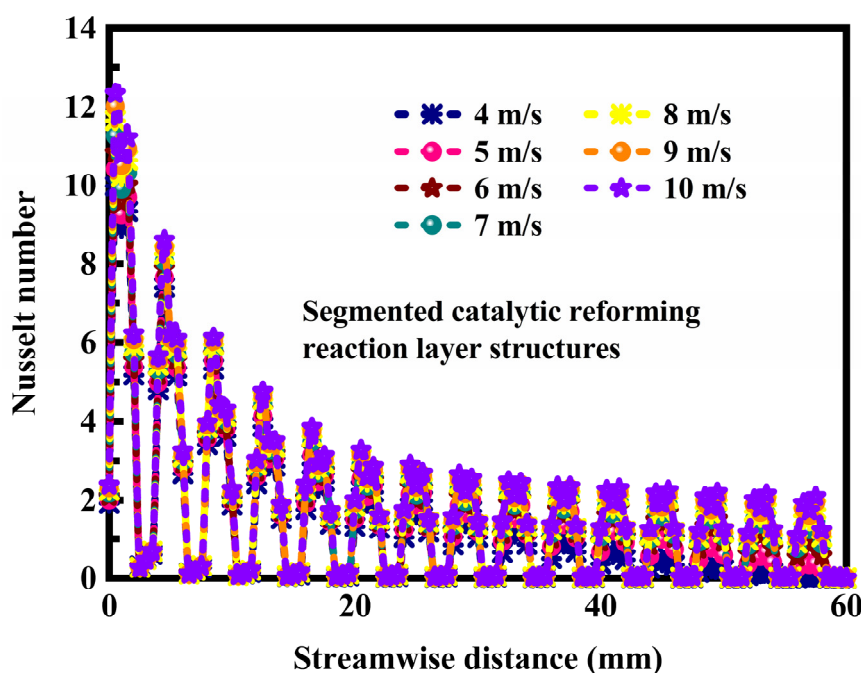


Figure 7. Nusselt number profiles along the length of the thermally integrated reformer with a segmented catalytic reforming reaction layer structure at different velocities of flow at the reactor inlet.

The Nusselt number profiles along the length of the thermally integrated reformer are presented in Figure 8 with different catalytic reaction layer structures. Although the transfer membrane can be provided in a variety of configurations, laminar and tubular membranes are preferred. Laminar membranes are generally employed in pairs which together constitute a membrane envelope, and the requisite zones are preferably provided by furrowing of the membrane surface in a direction transverse to the general direction of flow, although other configurations for the zones may be adopted if so desired. Laminar membranes, when extremely thin, require support for example from a sheet or the like possessing corrugations which define the ridges and furrows in the membrane. It is generally preferable for ridges and furrows in the laminar membranes constituting a membrane envelope to be located opposite each other without significant displacement. The corrugated sheet which may be rigid and formed for example from a plastics material by extrusion, pressing or molding is conveniently provided with substantially planar portions at, or in the region of, two or more edges thereof, the surface of which portions serve to space the ridges in the sheet from those of its neighbor. The latter portions are preferably integral with the sheet. A membrane envelope may be secured between the portions of two adjacent sheets by mechanical pressure applied thereto and preferably with the use of adhesive applied between the envelope and the portions. Adhesive is also preferably applied in the ridges of the sheet and the

membranes. In such cases, the membrane may be furrowed before commencement of fluid flow thereacross but preferably the membrane is planar or only slightly furrowed before introduction of pressurized fluid to the surface thereof which forces the membrane into corrugations in the sheet to form adequate furrows therein. When tubular membranes are employed, which membranes are preferably circular in cross section, the zones are preferably provided by circumferential furrowing. Although the latter configuration for the zones is preferred, others may be employed if so desired. With tubular membranes it may be found particularly convenient to employ a shaped member in the conduit to provide convenient to employ a shaped member in the conduit to provide zones in the region of the membrane surface. The member may for example be a rod or tube possessing circumferential ridges along the length thereof. When in place within the conduit the zones between the ridges are located in the region of the membrane surface and are hence associated therewith.

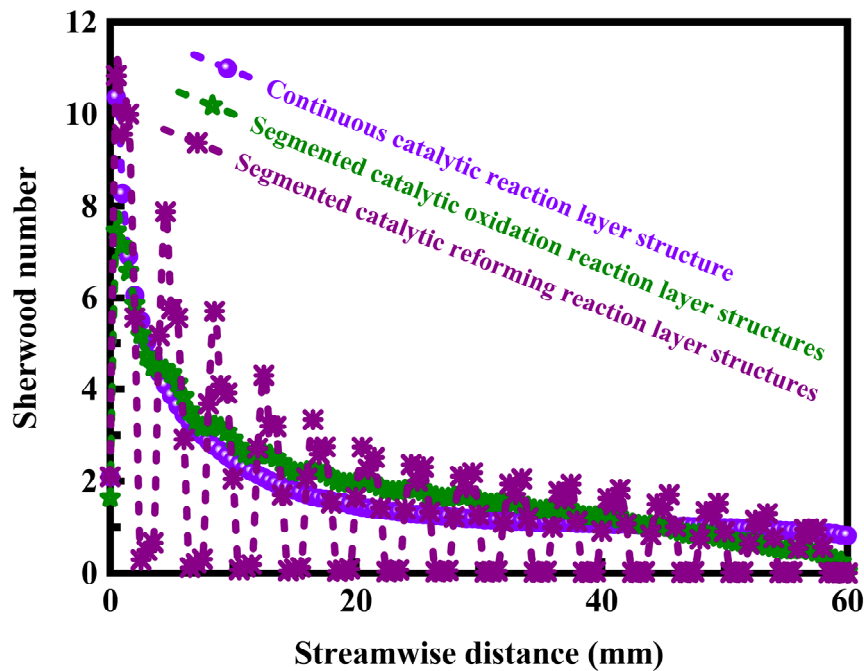


Figure 8. Nusselt number profiles along the length of the thermally integrated reformer with different catalytic reaction layer structures.

4. Conclusions

Numerical simulations are performed using computational fluid dynamics to better understand the characteristics of heat and mass transport in catalytic reaction layers of thermally integrated reformers. The present study aims to provide a fundamental understanding of the heat and mass transport in catalytic reaction layers of thermally integrated reformers. Particular emphasis is placed upon the Sherwood and Nusselt numbers involved in thermally integrated reformer with different catalytic reaction layer structures. The major conclusions are summarized as follows:

- A vapor-liquid equilibrium exists when the escape tendency of the specie from liquid to a vapor phase is exactly balanced with the escape phase at the same temperature and pressure.
- It may be beneficial to utilize the thermodynamic work potential provided by the transfer of heat, whereby the hot input stream is tagged as a heat source and the cold input stream is tagged as a heat sink, to drive the separation process in the desired direction, the entire process occurring in one operation.
- If a chamber partition operates below its maximum heat transfer flux capability, this flux often can be increased by augmenting adjacent latent energy transfer which transfers through the partition as sensible energy.

- The external balance establishes the net enthalpy offset and therefore the temperature difference between the two chambers and the net amount of liquid that may be evaporated or condensed.
- A pure diffusive heat and mass transport would lead to an uneven reaction density or current density in the catalytic reaction layer, on account of a corresponding lack of uniformity in the heat and mass transport in the same catalytic reaction layer.
- A high pressure drop in the thermally integrated reformer is to be avoided, since a high-pressure drop is associated with correspondingly high-power losses, which in turn results in a low overall efficiency.
- The conduit surface may vary along the general direction of flow to provide the zones either intermittently or preferably continuously as with an undulating membrane surface.
- When tubular membranes are employed, which membranes are preferably circular in cross section, the zones are preferably provided by circumferential furrowing.

References

- [1] G. Athanasaki, A. Jayakumar, and A.M. Kannan. Gas diffusion layers for PEM fuel cells: Materials, properties and manufacturing - A review. *International Journal of Hydrogen Energy*, Volume 48, Issue 6, 2023, Pages 2294-2313.
- [2] B. Amani and A. Zanj. Analysis of the effects of the gas diffusion layer properties on the effectiveness of baffled flow channels in improving proton exchange membrane fuel cells performance. *International Communications in Heat and Mass Transfer*, Volume 140, 2023, Article Number: 106558.
- [3] D. Niblett, V. Niasar, S. Holmes, A. Mularczyk, J. Eller, R. Prosser, and M. Mamlouk. Water cluster characteristics of fuel cell gas diffusion layers with artificial microporous layer crack dilation. *Journal of Power Sources*, Volume 555, 2023, Article Number: 232383.
- [4] W. Yoshimune, S. Kato, M. Inagaki, and S. Yamaguchi. A simple method to measure through-plane effective gas diffusivity of a gas diffusion layer for polymer electrolyte fuel cells. *International Journal of Heat and Mass Transfer*, Volume 191, 2022, Article Number: 122887.
- [5] A.T. Ertürk, U. Ergin, T. Kadioglu, A.C. Türkmen, and C. Çelik. Metal foams as a gas diffusion layer in direct borohydride fuel cells. *International Journal of Hydrogen Energy*, Volume 47, Issue 55, 2022, Pages 23373-23380.
- [6] P. Sarkezi-Selsky, H. Schmies, A. Latz, and T. Jahnke. Lattice Boltzmann simulation of liquid water transport in gas diffusion layers of proton exchange membrane fuel cells: Impact of gas diffusion layer and microporous layer degradation on effective transport properties. *Journal of Power Sources*, Volume 556, 2023, Article Number: 232415.
- [7] J. Sim, M. Kang, and K. Min. Effects of porosity gradient and average pore size in the in-plane direction and disposition of perforations in the gas diffusion layer on the performance of proton exchange membrane fuel cells. *Journal of Power Sources*, Volume 544, 2022, Article Number: 231912.
- [8] M. Kang, J. Sim, and K. Min. Analysis of surface and interior degradation of gas diffusion layer with accelerated stress tests for polymer electrolyte membrane fuel cell. *International Journal of Hydrogen Energy*, Volume 47, Issue 68, 2022, Pages 29467-29480.
- [9] G.H. Kim, D. Kim, J. Kim, H. Kim, and T. Park. Impact of cracked gas diffusion layer on performance of polymer electrolyte membrane fuel cells. *Journal of Industrial and Engineering Chemistry*, Volume 91, 2020, Pages 311-316.
- [10] C. Csoklich, M. Sabharwal, T.J. Schmidt, and F.N. Büchi. Does the thermal conductivity of gas diffusion layer matter in polymer electrolyte fuel cells? *Journal of Power Sources*, Volume 540, 2022, Article Number: 231539.

- [11] I.S. Lim, Y.I. Lee, B. Kang, J.Y. Park, and M.S. Kim. Electrochemical performance and water management investigation of polymer electrolyte membrane fuel cell (PEMFC) using gas diffusion layer with polytetrafluoroethylene (PTFE) content gradients in through-plane direction. *Electrochimica Acta*, Volume 421, 2022, Article Number: 140509.
- [12] M. Nasu, H. Yanai, N. Hirayama, H. Adachi, Y. Kakizawa, Y. Shirase, H. Nishiyama, T. Kawamoto, J. Inukai, T. Shinohara, H. Hayashida, and M. Watanabe. Neutron imaging of generated water inside polymer electrolyte fuel cell using newly-developed gas diffusion layer with gas flow channels during power generation. *Journal of Power Sources*, Volume 530, 2022, Article Number: 231251.
- [13] C. Carral and P. Mele. Modeling the original and cyclic compression behavior of non-woven gas diffusion layers for fuel cells. *International Journal of Hydrogen Energy*, Volume 47, Issue 55, 2022, Pages 23348-23359.
- [14] H. Pourrahmani and J.V. Herle. Water management of the proton exchange membrane fuel cells: Optimizing the effect of microstructural properties on the gas diffusion layer liquid removal. *Energy*, Volume 256, 2022, Article Number: 124712.
- [15] D. Zapardiel and P.A. García-Salaberri. Modeling the interplay between water capillary transport and species diffusion in gas diffusion layers of proton exchange fuel cells using a hybrid computational fluid dynamics formulation. *Journal of Power Sources*, Volume 520, 2022, Article Number: 230735.
- [16] M. Sarker, M.A. Rahman, F. Mojica, S. Mehrazi, W.J.M. Kort-Kamp, and P.-Y.A. Chuang. Experimental and computational study of the microporous layer and hydrophobic treatment in the gas diffusion layer of a proton exchange membrane fuel cell. *Journal of Power Sources*, Volume 509, 2021, Article Number: 230350.
- [17] S. Sakaida, Y. Takahashi, K. Tanaka, and M. Konno. Improvement of polymer electrolyte fuel cell performance by gas diffusion layer with relatively hydrophilic surface. *Journal of Power Sources*, Volume 518, 2022, Article Number: 230730.
- [18] M. Khatoonabadi, M.A. Safi, N.I. Prasianakis, J. Roth, J. Mantzaras, N. Kirov, and F.N. Büchi. Insights on the interaction of serpentine channels and gas diffusion layer in an operating polymer electrolyte fuel cell: Numerical modeling across scales. *International Journal of Heat and Mass Transfer*, Volume 181, 2021, Article Number: 121859.
- [19] P. Padavu, P.K. Koorata, and S.D. Bhat. Numerical investigation on the improved reactant mass transport with depth-dependent flow fields in polymer electrolyte fuel cell under inhomogeneous gas diffusion layer compression. *International Journal of Heat and Mass Transfer*, Volume 180, 2021, Article Number: 121796.
- [20] B.K. Kanchan, P. Randive, and S. Pati. Implications of non-uniform porosity distribution in gas diffusion layer on the performance of a high temperature PEM fuel cell. *International Journal of Hydrogen Energy*, Volume 46, Issue 35, 2021, Pages 18571-18588.
- [21] S. Cruz-Manzo and P. Greenwood. Low frequency inductive loop in EIS measurements of an open-cathode polymer electrolyte fuel cell stack. Impedance of water vapour diffusion in the cathode catalyst layer. *Journal of Electroanalytical Chemistry*, Volume 900, 2021, Article Number: 115733.
- [22] A. Alrashidi and H. Liu. Laser-perforated anode gas diffusion layers for direct methanol fuel cells. *International Journal of Hydrogen Energy*, Volume 46, Issue 34, 2021, Pages 17886-17896.
- [23] W. Yoshimune, S. Kato, and S. Yamaguchi. Multi-scale pore morphologies of a compressed gas diffusion layer for polymer electrolyte fuel cells. *International Journal of Heat and Mass Transfer*, Volume 152, 2020, Article Number: 119537.
- [24] P.-Y.A. Chuang, M.A. Rahman, F. Mojica, D.S. Hussey, D.L. Jacobson, and J.M. LaManna. The interactive effect of heat and mass transport on water condensation in the gas diffusion layer of a proton exchange membrane fuel cell. *Journal of Power Sources*, Volume 480, 2020, Article Number:

229121.

- [25] P.A. García-Salaberri. Modeling diffusion and convection in thin porous transport layers using a composite continuum-network model: Application to gas diffusion layers in polymer electrolyte fuel cells. *International Journal of Heat and Mass Transfer*, Volume 167, 2021, Article Number: 120824.
- [26] S.-H. Lee, J.H. Nam, C.-J. Kim, and H.M. Kim. Effect of fiber orientation on Liquid-Gas flow in the gas diffusion layer of a polymer electrolyte membrane fuel cell. *International Journal of Hydrogen Energy*, Volume 46, Issue 68, 2021, Pages 33957-33968.
- [27] F. Bezzo, S. Macchietto, and C.C. Pantelides. A general framework for the integration of computational fluid dynamics and process simulation. *Computers & Chemical Engineering*, Volume 24, Issues 2-7, 2000, Pages 653-658.
- [28] A. Brucato, M. Ciofalo, F. Grisafi, and R. Tocco. On the simulation of stirred tank reactors via computational fluid dynamics. *Chemical Engineering Science*, Volume 55, Issue 2, 2000, Pages 291-302.
- [29] C.A. Serra, M.R. Wiesner, and J.-M. Laine. Rotating membrane disk filters: Design evaluation using computational fluid dynamics. *Chemical Engineering Journal*, Volume 72, Issue 1, 1999, Pages 1-17.
- [30] M. Bistolfi, N. Mancini, and F. Podenzani. Computational fluid dynamics modelling of multiphase reactors. *Computer Aided Chemical Engineering*, Volume 8, 2000, Pages 379-384.
- [31] R. Rieger, C. Weiss, G. Wigley, H.-J. Bart, and R. Marr. Investigating the process of liquid-liquid extraction by means of computational fluid dynamics. *Computers & Chemical Engineering*, Volume 20, Issue 12, 1996, Pages 1467-1475.
- [32] C.K. Harris, D. Roekaerts, F.J.J. Rosendal, F.G.J. Buitendijk, P. Daskopoulos, A.J.N. Vreenegoor, and H. Wang. Computational fluid dynamics for chemical reactor engineering. *Chemical Engineering Science*, Volume 51, Issue 10, 1996, Pages 1569-1594.
- [33] R.O. Fox. On the relationship between Lagrangian micromixing models and computational fluid dynamics. *Chemical Engineering and Processing: Process Intensification*, Volume 37, Issue 6, 1998, Pages 521-535.
- [34] M. Azaiez, S. Boudoux-Dagonat, M.A. Fikri, and G. Labrosse. The computational fluid dynamics by spectral methods: Some illustrative results. *Computers & Chemical Engineering*, Volume 17, Supplement 1, 1993, Pages S523-S529.
- [35] J. Bode. Computational fluid dynamics applications in the chemical industry. *Computers & Chemical Engineering*, Volume 18, Supplement 1, 1994, Pages S247-S251.
- [36] A.D. Gosman. Developments in industrial computational fluid dynamics. *Chemical Engineering Research and Design*, Volume 76, Issue 2, 1998, Pages 153-161.
- [37] V.M.T.M. Silva and A.E. Rodrigues. Kinetic studies in a batch reactor using ion exchange resin catalysts for oxygenates production: Role of mass transfer mechanisms. *Chemical Engineering Science*, Volume 61, Issue 2, 2006, Pages 316-331.
- [38] S. Matthes, T. Merbach, J. Fitschen, M. Hoffmann, and M. Schlüter. Influence of counterdiffusion effects on mass transfer coefficients in stirred tank reactors. *Chemical Engineering Journal Advances*, Volume 8, 2021, Article Number: 100180.
- [39] M. Fechtner and A. Kienle. Wave reflections in counter-current separation processes with unequal mass transfer coefficients. *Chemical Engineering Science*, Volume 260, 2022, Article Number: 117929.
- [40] J. Guarco, H. Harmuth, and S. Vollmann. Method for determination of mass transfer coefficients for dissolution of dense ceramics in liquid slags. *International Journal of Heat and Mass Transfer*, Volume 186, 2022, Article Number: 122494.
- [41] H.N. Vu, X.L. Nguyen, J. Han, and S. Yu. A study on vapor transport characteristics in hollow-fiber

- membrane humidifier with empirical mass transfer coefficient. *International Journal of Heat and Mass Transfer*, Volume 177, 2021, Article Number: 121549.
- [42] E.M. Lakhdissi, A. Fallahi, C. Guy, and J. Chaouki. Effect of solid particles on the volumetric gas liquid mass transfer coefficient in slurry bubble column reactors. *Chemical Engineering Science*, Volume 227, 2020, Article Number: 115912.
- [43] T. Deleau, M.H.H. Fechter, J.-J. Letourneau, S. Camy, J. Aubin, A.S. Braeuer, and F. Espitalier. Determination of mass transfer coefficients in high-pressure two-phase flows in capillaries using Raman spectroscopy. *Chemical Engineering Science*, Volume 228, 2020, Article Number: 115960.
- [44] K.C. Sandeep, S. Mohan, D. Mandal, and S. Mahajani. Determination of gas film mass transfer coefficient in a packed bed reactor for the catalytic combustion of hydrogen. *Chemical Engineering Science*, Volume 202, 2019, Pages 508-518.
- [45] M. Fechtner and A. Kienle. Approximate shock layer solutions for the separation of multicomponent mixtures with different axial dispersion or mass transfer coefficients. *Chemical Engineering Science*, Volume 231, 2021, Article Number: 116335.
- [46] A.D. Pérez, B.V.D. Bruggen, and J. Fontalvo. Study of overall mass transfer coefficients in a liquid membrane in Taylor flow regime: Calculation and correlation. *Chemical Engineering and Processing - Process Intensification*, Volume 134, 2018, Pages 20-27.
- [47] K. Scott, W.M. Taama, P. Argyropoulos, and K. Sundmacher. The impact of mass transport and methanol crossover on the direct methanol fuel cell. *Journal of Power Sources*, Volume 83, Issues 1-2, 1999, Pages 204-216.
- [48] M. Wöhr, K. Bolwin, W. Schnurnberger, M. Fischer, W. Neubrand, and G. Eigenberger. Dynamic modelling and simulation of a polymer membrane fuel cell including mass transport limitation. *International Journal of Hydrogen Energy*, Volume 23, Issue 3, 1998, Pages 213-218.
- [49] D. Singh, D.M. Lu, and N. Djilali. A two-dimensional analysis of mass transport in proton exchange membrane fuel cells. *International Journal of Engineering Science*, Volume 37, Issue 4, 1999, Pages 431-452.
- [50] K. Scott, W.M. Taama, S. Kramer, P. Argyropoulos, and K. Sundmacher. Limiting current behaviour of the direct methanol fuel cell. *Electrochimica Acta*, Volume 45, Issue 6, 1999, Pages 945-957.
- [51] A. Khalidi, B. Lafage, P. Taxil, G. Gave, M.J. Clifton, and P. Cézac. Electrolyte and water transfer through the porous electrodes of an immobilised-alkali hydrogen-oxygen fuel cell. *International Journal of Hydrogen Energy*, Volume 21, Issue 1, 1996, Pages 25-31.
- [52] K. Scott, P. Argyropoulos, and K. Sundmacher. A model for the liquid feed direct methanol fuel cell. *Journal of Electroanalytical Chemistry*, Volume 477, Issue 2, 1999, Pages 97-110.
- [53] D. Chu and R. Jiang. Comparative studies of polymer electrolyte membrane fuel cell stack and single cell. *Journal of Power Sources*, Volume 80, Issues 1-2, 1999, Pages 226-234.
- [54] A.S. Aricò, P. Cretì, V. Baglio, E. Modica, and V. Antonucci. Influence of flow field design on the performance of a direct methanol fuel cell. *Journal of Power Sources*, Volume 91, Issue 2, 2000, Pages 202-209.
- [55] H. Dohle, J. Divisek, and R. Jung. Process engineering of the direct methanol fuel cell. *Journal of Power Sources*, Volume 86, Issues 1-2, 2000, Pages 469-477.
- [56] J. Cunha and J.L.T. Azevedo. Modelling the integration of a compact plate steam reformer in a fuel cell system. *Journal of Power Sources*, Volume 86, Issues 1-2, 2000, Pages 515-522.
- [57] D. Benavente, M.A.G.D. Cura, R. Fort, and S. Ordóñez. Thermodynamic modelling of changes induced by salt pressure crystallisation in porous media of stone. *Journal of Crystal Growth*, Volume 204, Issues 1-2, 1999, Pages 168-178.
- [58] M. Awartani and M.H. Hamdan. Non-reactive gas-particulate models of flow through porous media. *Applied Mathematics and Computation*, Volume 100, Issue 1, 1999, Pages 93-102.

- [59]J. Bergendahl and D. Grasso. Prediction of colloid detachment in a model porous media: Hydrodynamics. *Chemical Engineering Science*, Volume 55, Issue 9, 2000, Pages 1523-1532.
- [60]Q.S. Chen, V. Prasad, A. Chatterjee, and J. Larkin. A porous media-based transport model for hydrothermal growth. *Journal of Crystal Growth*, Volumes 198-199, Part 1, 1999, Pages 710-715.
- [61]T. Masuoka and Y. Takatsu. Turbulence model for flow through porous media. *International Journal of Heat and Mass Transfer*, Volume 39, Issue 13, 1996, Pages 2803-2809.
- [62]X. Lu, P. Xie, D.B. Ingham, L. Ma, and M. Pourkashanian. A porous media model for CFD simulations of gas-liquid two-phase flow in rotating packed beds. *Chemical Engineering Science*, Volume 189, 2018, Pages 123-134.
- [63]T. Santagata, R. Solimene, G. Aprea, and P. Salatino. Modelling and experimental characterization of unsaturated flow in absorbent and swelling porous media. *Chemical Engineering Science*, Volume 224, 2020, Article Number: 115765.
- [64]P. Gurikov, A. Kolnoochenko, M. Golubchikov, N. Menshutina, and I. Smirnova. A synchronous cellular automaton model of mass transport in porous media. *Computers & Chemical Engineering*, Volume 84, 2016, Pages 446-457.
- [65]M. Veyskarami, A.H. Hassani, and M.H. Ghazanfari. Modeling of non-Darcy flow through anisotropic porous media: Role of pore space profiles. *Chemical Engineering Science*, Volume 151, 2016, Pages 93-104.
- [66]B.R. Becker and B.A. Fricke. Modeling transport processes in heat and mass releasing porous media. *International Communications in Heat and Mass Transfer*, Volume 24, Issue 3, 1997, Pages 439-448.